

ÇANKAYA UNIVERSITY
GRADUATE SCHOOL OF NATURAL AND APPLIED SCIENCES
ELECTRONIC AND COMMUNICATION ENGINEERING

MASTER THESIS

DRIVER DESIGN FOR ASYNCHRONOUS MOTORS:
DIGITAL SIGNAL PROCESSING, CONTROL AND DATA
ACQUISITION

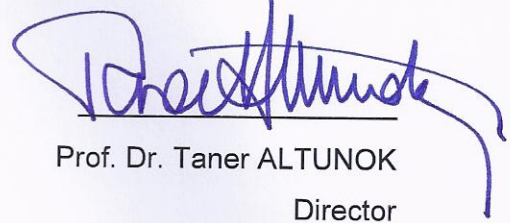
HABİB ÖZER ÖZ

OCTOBER, 2012

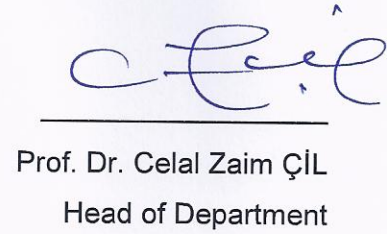
Title of the Thesis: **Driver Design for Asynchronous Motors: Digital Signal Processing, Control and Data Acquisition**

Submitted By: **Habib Özer Öz**

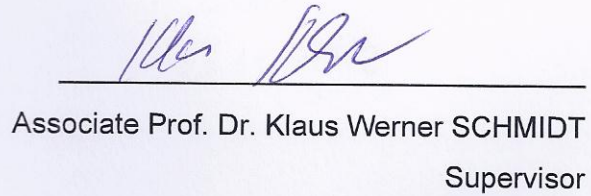
Approval of the Graduate School of Natural and Applied Sciences


Prof. Dr. Taner ALTUNOK
Director

I certify that this thesis satisfies all the requirements as a thesis for the degree of Master of Science.


Prof. Dr. Celal Zaim ÇİL
Head of Department

This is to certify that we have read this thesis and that in our opinion it is fully adequate, in scope and quality, as a thesis for the degree of Master of Science.


Associate Prof. Dr. Klaus Werner SCHMIDT
Supervisor

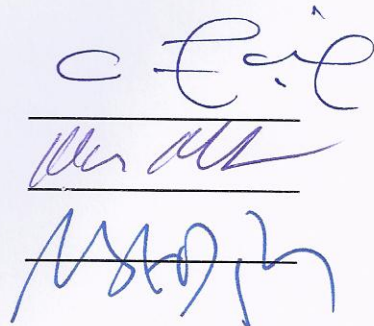
Examination Date : 12.10.2012

Examining Committee Members:

Prof. Dr. Celal Zaim ÇİL (Çankaya Univ.)

Associate Prof. Dr. Klaus SCHMIDT (Çankaya Univ.)


Assistant Prof. Dr. Mustafa DOĞAN (Doğuş Univ.)



STATEMENT OF NON-PLAGIARISM

I hereby declare that all information in this document has been obtained and presented in accordance with academic rules and ethical conduct. I also declare that, as required by these rules and conduct, I have fully cited and referenced all material and results that are not original to this work.

Name, Last Name : HABİB ÖZER ÖZ

Signature : 

Date : 13.11.2012

ABSTRACT

DRIVER DESIGN FOR ASYNCHRONOUS MOTORS: DIGITAL SIGNAL PROCESSING, CONTROL AND DATA ACQUISITION

ÖZ, Habib Özer

M.Sc., Department of Electronics and Communication Engineering

Supervisor: Associate Prof. Dr. Klaus SCHMIDT

September 2012, 83 Pages

In this research, a three-phase AC induction motor driver training set is designed for students and educators. The AC induction motor driver training set design consists of two main parts: the power electronic part and the system control part. The main components of the power electronic part are the rectifier and the inverter. The rectifier generates a DC voltage supply for feeding the inverter. In the thesis, it is realized both as a controlled and an uncontrolled rectifier. The inverter generates a three-phase AC voltage in order to drive the AC induction motor. As one main contribution of the thesis, the power electronic part is realized such that all relevant signals can be measured and analyzed for educational purposes. The system control part uses the F28035 DSP for computations. V/F control is implemented with the space vector modulation method for open-loop speed control. In addition, closed-loop speed control is performed based on a system plant model, that is found with the help of MATLAB. Finally, a new method for controlling the maximum available torque is realized. The study is supported by various measurement experiments that are obtained using the data acquisition system D-LAB.

Keywords: Three-phase Motor Driver, Asynchronous Motor, Power Electronics, Control, DSP, System Integration,

ÖZ

ASENKRON MOTORLAR için SÜRÜCÜ TASARIMI: SAYISAL SİNYAL İŞLEME, KONTROL ve VERİ TOPLAMA

ÖZ, Habib Özer

Yüksek Lisans, Elektronik ve Haberleşme Mühendisliği Anabilim Dalı

Tez Yöneticisi: Doç. Dr. Klaus SCHMIDT

Eylül 2012, 83 Sayfa

Bu çalışmada öğrenciler ve eğitimciler için üç faz AC indüksiyon motor sürücüsü eğitim seti tasarlanmıştır. AC indüksiyon motor sürücüsü eğitim seti iki ana kısımdan oluşur. Bu kısımlar güç elektroniği ve sistem kontrolü kısımlarıdır. Güç elektroniği kısmı doğrultma ve sürücü olmak üzere iki alt kısımdan oluşur. Doğrultma alt kısmı, sürücü için gereken DC gerilimi oluşturur. Bu DC gerilimi oluşturmak için kontrollü ve kontrolsüz doğrultucular tasarlanmıştır. Sürücü alt kısmı AC indüksiyon motorunu sürmek için üç faz AC gerilim oluşturur. Bu çalışmanın ana katkılarından biri olan güç elektroniği kısmında eğitim amaçlı tüm sinyaller ölçülüp, analiz edilebilir. Sistem kontrol kısmı F28035 sayısal sinyal işlemcisi kullanır. Motor açık döngü hız kontrolü için uzay vektör modülasyon methodu ile birlikte V/F kontrolü uygulanmıştır. Yine bu çalışma kapsamında, kapalı devre hız kontrolü MATLAB yardımıyla bulunan sistem modeline göre gerçekleştirilmiştir. Son olarak, maksimum torku kontrol etmek için yeni bir yöntem gerçekleştirilmiştir. Bu çalışmada veri toplama sistemi olarak D-LAB ürünü kullanılmıştır.

Anahtar Kelimeler: Üç Faz Motor Sürücüsü, Asenkron Motor, Güç Elektroniği, Kontrol, DSP, Sistem Entegrasyonu

ACKNOWLEDGEMENTS

The author wishes to express his deepest gratitude to his supervisor Associate Prof. Dr. Klaus SCHMIDT for his guidance, advice, criticism, encouragements and insight throughout the research. Also I would like to thank my father (Mehmet Sait Öz) and my family for their support.

TABLE OF CONTENTS

STATEMENT OF NON-PLAGIARISM	iii
ABSTRACT	iv
ÖZ	v
ACKNOWLEDGEMENTS	vi
TABLE OF CONTENTS	vii
CHAPTERS	
INTRODUCTION.....	1
1. BACKGROUND.....	4
1.1 RECTIFIER.....	4
1.2 INVERTER	5
1.3 AC MOTOR.....	6
1.4 MAGNETIC POWDER BRAKE	9
1.5 SENSORS FOR MOTOR CONTROL	9
1.6 MOTIVATION AND PROBLEM DEFINITION.....	10
1.7 DESIGN REQUIREMENTS / CRITERIA.....	10
2. IMPLEMENTATION.....	12
2.1 POWER ELECTRONIC MODULE DESIGN.....	13
2.1.1. Rectifier Design	13
2.1.2. Inverter Design	16
2.2 SYSTEM CONTROL MODULE DESIGN.....	23
2.2.1. Scalar Control	23
2.2.2. Space Vector Modulation Method.....	26
2.2.3. Control System Design	30
2.3 INTEGRATION.....	34

3. EVALUATION OF POWER ELECTRONICS MODULE	37
3.1 EVALUATION OF RECTIFIER SUBSYSTEM.....	37
3.2 EVALUATION OF INVERTER SUBSYSTEM	43
4. EVALUATION OF THE CONTROL MODULE.....	46
4.1 PLANT MODEL IDENTIFICATION.....	47
4.2 CONTROLLER DESIGN	52
4.2.1. Pole Placement Method.....	53
4.3 EVALUATION RESULTS OF THE SYSTEM	57
4.3.1. Behaviour of AC Induction Motor.....	57
4.3.2. Behaviour of The AC Induction Motor with Feedback Control...	59
4.3.3. Behaviour of The AC Induction Motor with Speed and Torque Control.....	61
5. CONCLUSION.....	66
REFERENCES.....	67
CURRICULUM VITAE.....	71

LIST OF FIGURES

Figure 1: Full wave single phase bridge rectifier	5
Figure 2: Basic Design of Three Phase Inverter	6
Figure 3: Induction Motor Rotor.....	8
Figure 4: Squirrel cage rotor AC induction motor cutaway view.....	8
Figure 5: Encoder Disk and Output Signal	9
Figure 6: Main Block Diagram of the System	12
Figure 7: Diode Module Design.....	13
Figure 8: Thyristor Module Design	14
Figure 9: Single Phase Rectifier DC Voltage Output with Thyristors	15
Figure 10: Single Phase Thyristor Controller Design	15
Figure 11: Three Phase Rectifier DC Voltage Output with Thyristors	16
Figure 12: Three Phase Thyristor Controller Module Design	17
Figure 13: Where MOSFETs and IGBTs are preferred.....	18
Figure 14: Block Diagram of 7MBP50RJ120 ^[17]	19
Figure 15: Isolated Four DC Supply Design.....	20
Figure 16: Isolated IGBT Drive Part	21
Figure 17: Isolated IGBTs Alarm Output Design.....	22
Figure 18: Inverter Card	23
Figure 19: Simplified steady-state equivalent circuit of induction motor.....	24
Figure 20: Stator Voltage vs Frequency Profile under V/F control	25
Figure 21: Torque vs Slip Speed of an Induction motor with Constant Stator Flux. 26	
Figure 22: Typical Three Phase VSI Diagram.....	27
Figure 23: The Basic Vectors and Switching States	29
Figure 24: V/F controlled Open Loop System	31
Figure 25: V/F controlled Open Loop system with speed measurement.....	32
Figure 26: V/F Controlled Closed Loop System with Speed Sensor.....	33
Figure 27: DC Supply Input Control for Closed Loop Torque Control	33
Figure 28: Translator Card Schematic Design	35
Figure 29: Translator Card PCB Design.....	36
Figure 30: Translator Card	36

Figure 31: Single Phase Rectifier Test Circuit.....	37
Figure 32: Single Phase Rectifier Output Voltage Without Capacitor	38
Figure 33: Single Phase Rectifier Output Voltage With Capacitor	38
Figure 34: Three Phase Rectifier Test Circuit	39
Figure 35: Three Phase Rectifier Output Voltage Without Capacitor.....	39
Figure 36: Controlled Single Phase Rectifier Test Circuit	40
Figure 37: Controllable Single Phase Rectifier Output Voltage Without Capacitor .	41
Figure 38: Controllable Single Phase Rectifier Output Voltage with Capacitor.....	41
Figure 39: Controlled Three Phase Rectifier Test Circuit.....	42
Figure 40: Controllable Three Phase Rectifier Output Voltage Without Capacitor..	42
Figure 41: Star Connection for AC induction Motor.....	43
Figure 42: Inverter Output Voltage (Line to Neutral)	44
Figure 43: Delta Connection for AC Induction Motor.....	44
Figure 44: Inverter Voltage Output (Line-to-Line).....	45
Figure 45: PWM Signals (Upper Side IGBT) for Controlling the Inverter	46
Figure 46: Desired Phase Frequency Graph (Plant Input) for Acceleration	48
Figure 47: Motor Speed Graph (Plant Output) for Acceleration	48
Figure 48: Output of The MATLAB Identification Fitting Tool.....	49
Figure 49: Open Loop System Step Response.....	50
Figure 50: Plant Model Validation	50
Figure 51: AC Induction Motor Step Response.....	51
Figure 52: Differences of The AC Induction Motor and Plant Model	51
Figure 53: A Basic Feedback Control System.....	52
Figure 54: The Ideal PID Controller.....	53
Figure 55: Unit Step Response	54
Figure 56: The Step Response of Closed Loop System	55
Figure 57: Closed Loop System Output with PID Control	56
Figure 58: Simulation and Real Time System Validation	56
Figure 59: Open-Loop System with Disturbance.....	57
Figure 60: Behaviour of the AC Motor under a Few Load.....	58
Figure 61: Behaviour of the AC Motor under High Load	58
Figure 62: Closed-Loop System with Disturbance	59
Figure 63: Behaviour of the AC Motor with the Speed Controller under a Small Load	60
Figure 64: Behaviour of the AC Motor with the Speed Controller under Critical Load.....	60

Figure 65: Behaviour of the AC Motor with the Torque Controller under a Small Load..... 63

Figure 66: Behaviour of the AC Motor with the Speed and Torque Controllers under the Critical Load..... 63

Figure 67: Behaviour of the AC Motor with the Speed and Torque Controllers under High Load 65

INTRODUCTION

AC induction motors are the most widely used type of motor. The reasons for this are higher robustness, higher reliability, lower prices and higher efficiency (up to 80%) in comparison with other motor types.^[1] Each AC motor type has different maximum speed and torque values. In AC motor, maximum torque is changed by the input voltage of AC motor. Also speed is changed by the frequency of AC motor power supply. AC induction motor's speed and torque control require the use of inverter. For this reason AC induction motor's driver design is an important area of research as well as student training.

Nowadays training sets are important for technical education. Accordingly, experimental platforms are designed in order to understand the industrial product design. These platforms are supposed to address different training issues. In the literature, different kinds of training sets are available. Unfortunately, the common training sets directly use industrial products in the system design. In this case, the training platform is not suitable for many aspects of engineering education. The reasons are that industrial products are a packaged end product. Hence, students can not access the interior architecture of such products. It is not possible to observe the relevant signals in the system and it is not possible to change the embedded software. For example, the company Yıldırım Elektronik has a power electronic training set which uses the industrial motor driver (ACS355) for the inverter experiments [49]. Hence, this platform does not support all aspects of power electronic education. Differently, the company Leybold Didactic offers a power electronic set with both an industrial motor driver and a custom-made motor driver for inverter experiments. In this set, the industrial motor driver is taught as a compact motor driver unit. In addition, the custom-made motor driver is taught in order to study the design of AC motor drivers. However, this training set is lacking in terms of system modeling and simulation. Moreover, it does not support experiments for the speed and torque control of AC induction motors. Because of

this reason, the AC induction motor driver and control training set design is selected for this study with the help of the company Yıldırım Elektronik.

In accordance with the previous discussion, the research in this thesis is interested in developing a three phase inverter training set for experiments in basic power electronic theory as well as feedback control. In the power electronics training, it is essential that students understand the operation of power electronic components and their design. Because of that reason students need a dedicated experimental platform for studying AC induction motor drivers. In principle, such training set consists of a rectifier part, an inverter part, a controller part and the AC induction motor for conducting power electronics experiments. In addition, the application of control suggests the usage of a torquemeter (torque measurements), an encoder (speed measurements) and a magnetic powder brake (load torque disturbance).

In this study, the training set is supported by simulation work. MATLAB is used for finding the system plant model and PID controller design by the pole placement method is used to realize feedback control. The control design is validated both by simulation and measurements in the real hardware system.

The thesis is organized as follows. Chapter 1 gives the background of this study. In Section 1.1, rectifiers are described in a simple way. In Section 1.2, three phase inverters are discussed And in Section 1.3, asynchronous AC induction motors are explained. In Section 1.4, the operation of the magnetic powder brake is described. Section 1.5 explains which kind of sensors are used for motor control. In Section 1.6, motivation and problem definition is explained for this study. Section 1.7 shows the selected design requirements and criteria for this study. Chapter 2 describes how to implement sub-systems for this study. Chapter 2 consists of the power electronic module design (Section 2.1), the system control module design (Section 2.2) and the integration (Section 2.3). Section 2.1 describes the rectifier design (Section 2.1.1) and the inverter design (Section 2.1.2). Also Section 2.2 describes the scalar control (Section 2.2.1), space vector modulation method (Section 2.2.2) and control system design (Section 2.2.3). Chapter 3 focuses on the evaluation of the power electronic module. This chapter shows the signal output of the power electronic subsystems. Also this chapter consists of the evaluation of rectifier subsystem (Section 3.1) and the evaluation of the inverter subsystem (Section 3.2). Chapter 4 consists of the plant model identification (Section 4.1), the controller design (Section 4.2) and the evaluation results of the system (Section 4.3). In

Section 4.2.1, pole placement method is used for the controller design. Also Section 4.3 evaluates the behaviour of the AC induction motor (Section 4.3.1), the behaviour of the AC induction motor with the feedback control (Section 4.3.2) and the behaviour of the AC induction motor with speed and torque control (Section 4.3.3). Finally, Chapter 5 gives conclusions.

CHAPTER I

BACKGROUND

The functions of the main parts of the inverter system will be learned in this chapter. For this reason, sub-parts, which are used in this research, are described in a simple way. The main working principles are explained for each sub-parts. Hence, motivation and problem definition is explained. After that, the selected design requirements and criteria are shown.

1.1 RECTIFIER

The rectifier converts AC voltage to DC voltage. Normally it uses diodes for rectifying AC voltage. If diodes are used in the rectifier design, the DC voltage gain can not be controlled. For controlling the DC voltage gain, it is beneficial to use a thyristor in the rectifier design. In principle, the types of rectifiers are half wave rectifier and full wave rectifier. For example, a full wave single phase bridge rectifier design has 4 diodes. In Figure 1, diodes 1/3 and 2/4 run at the same time. When the AC voltage is positive, 1/3 diodes run. On the other hand if the AC voltage is negative, diodes 2/4 run. It has to be noted that the output of the full wave single phase bridge rectifier is not a smooth DC voltage. When a capacitor is connected, output of the full wave rectifier becomes smooth DC voltage. In the scope of this thesis, four different types of rectifiers are designed. They are uncontrolled single phase rectifier, controlled single phase rectifier, uncontrolled three phase rectifier, controlled three phase rectifier. Rectifier part which is controlled by the controller part, controls the DC voltage amplitude. The rectifier part are designed modular so that connections of modules are changeable. For this reason all design can be analyzed by the students.^[26]

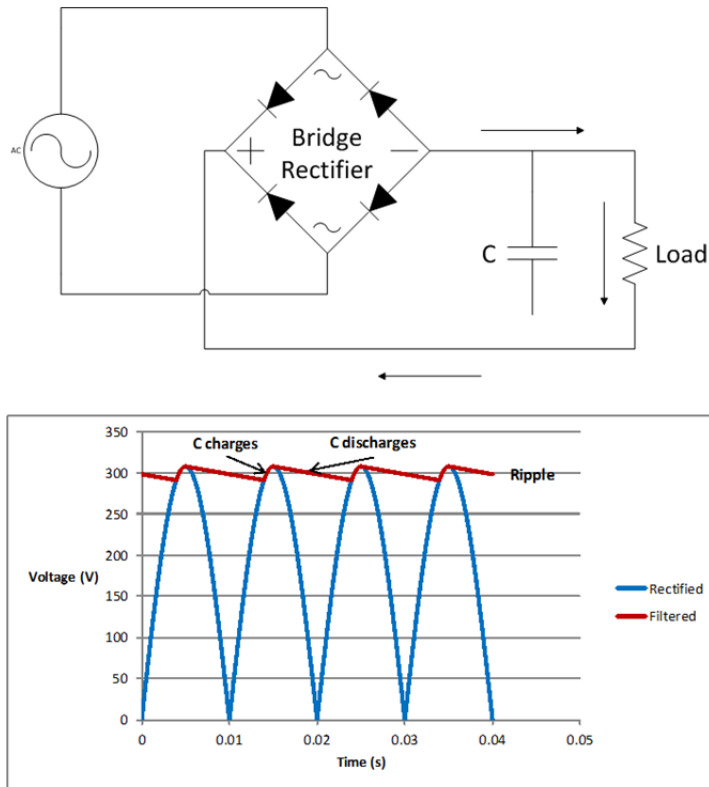


Figure 1: Full wave single phase bridge rectifier

1.2 INVERTER

The inverter converts DC voltage to AC voltage with high frequency switching. It can control the output of the AC voltage frequency. PWM (Pulse Width Modulation) signals are used for controlling the frequency. Normally a microcontroller is used for generating the PWM signal and PWM signals are applied to the semiconductor device's gate pins. A three phase inverter consists of 6 power semiconductor devices. Usually IGBT (Insulated Gate Bipolar Transistor) or MOSFET (metal oxide semiconductor field effect transistor) are used in the inverter design. The basic design of three phase inverter is shown in Figure 2. In this figure, 6 IGBTs are used. Each of the two vertical IGBTs generates a single phase voltage. Also each single phase has a 120° phase difference compared to the other phases. Together they generate three phase AC power supply.^[26]

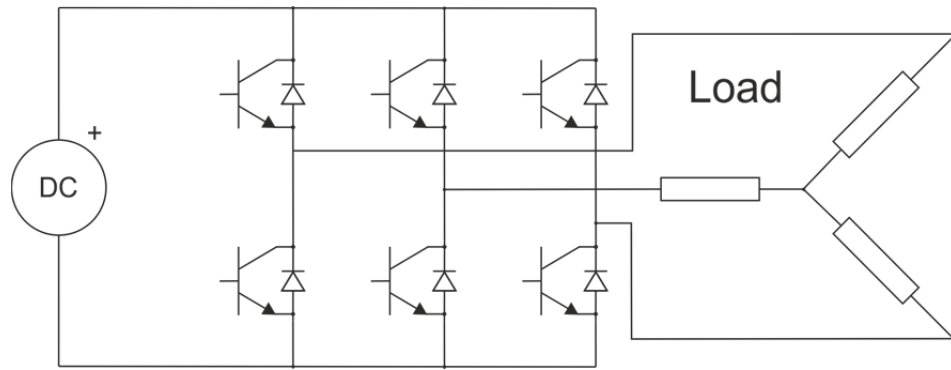


Figure 2: Basic Design of Three Phase Inverter

Nowadays Digital Signal Processors (DSP), which are special microprocessor that are optimized for the fast operational needs of digital signal processing, are used in inverter design. Even, some kind of DSP are optimized for motor control. Because of that they have ePWM (Enhanced Pulse Width Modulator), ADC (Analog-To-Digital Converter), QEP (Enhanced Quadrature Encoder Pulse), eCAP (Enhanced Capture) peripheral modules. DSPs can do complex mathematical operations. This is important for our research, because DSPs can implement complex control algorithm for driving AC induction motor.^{[39] [40] [41]}

1.3 AC MOTOR

The idea of converting electrical energy to mechanical movement was first claimed by Michael Faraday in 1821. He experimented that when current flows through a free hanging wire around a magnet, wire starts to rotate around magnet. First electrical motor, used in an industrial application, is developed by Emily and Thomas Davenport and patented in 1837. This motor was rotating about 600 revolutions per minute. The first successful DC motor was invented by Zenobe Gramme in 1873. Gramme used two dynamos instead of one. This motor led to commutator controlled DC motors. In 1886 Julien Sprague invented the modern DC motor. This motor was capable to work at constant speed at variable loads and can be controlled easily. Sprague engine started golden age for DC motors. By growing industry DC motors widely used for mass production.^{[26] [38] [45]}

The first successful AC motor was invented in 1888. Nicola Tesla, improved his machine with the help of Westinghouse Company. Despite being small sized and cost effective compared to DC motors, AC motors were not preferred in industry

untill late 20th century. Main reason was the efficiency problem. Efficiency on induction machine depends on the air gap between stator and rotor. This problem solved in time by developing production techniques of motors. But solving efficiency problem was not sufficient. Control of an AC motor is much harder than DC motor. Developing semiconductor technology, and production of cheaper control devices, make AC motors replace old fashioned DC motors.^{[38] [25]}

Since developed electric motor are indispensable for industry. Growing industry, needs to decrease production costs in competitive market. Today, almost all branches of industry prefer to use AC motors instead of DC motor. AC motors are smaller in shape, easy to produce, have lower maintenance costs, much more simple form and they are also cheaper than DC motors. More than fifty percent of produced electricity consumed by electric motors.^{[38] [45]}

These machines are both used for generating electricity from physical movement or generating rotation from electricity. In this thesis , electrical machine will be examined in motor mode.^[31]

Main principle of AC motor is following a rotating magnetic field. This can be achieved by generating a static magnetic field from stator windings and excite rotor with AC current. By this method, rotor magnetic field is generated by an outer source. Exciting rotor with an external source requires ring-brush mechanism. Alternate way is to generate rotating magnetic field at stator windings. Induction machines generate required rotor magnetic field from stator currents. Stator magnetic field induces current at shorted rotor winding. This magnetic field follows stator magnetic field and generates mechanical rotation.^[38]

Most widely used type of AC motor is squirrel cage motor. Main conductors, usually copper bars, are shorted at both ends with a metal bar as shown in Figure 3. Stator current generates a rotating magnetic field at a speed (ω_s). Changing magnetic fields creates a current at shorted rotor windings. Phase difference at stator winding current and induced rotor winding current causes rotation.^{[25] [31]}

After rotation begins, rotor starts to accelerate. Decreasing relative speed between stator magnetic field and rotor causes decreasing rotor currents. Decreasing rotor current, decreases the torque generated by motor. Hence, the motor reaches a

steady state equal to angular speed of the stator rotating magnetic field which is generally called synchronous speed if it is not loaded. If motor is loaded, motor reaches steady state at a lower speed than synchronous speed. Ratio between actual rotor speed and synchronous speed is called slip (s).^[45]

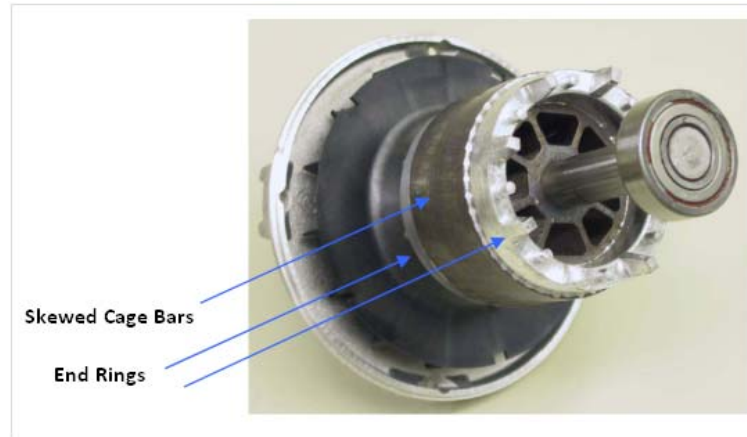


Figure 3: Induction Motor Rotor

In Figure 4 the rotor speed is denoted by Ω . Stator and rotor frequencies are linked by the slip s , expressed in per unit as $s = (\omega_s - \omega_r)/\omega_s$.

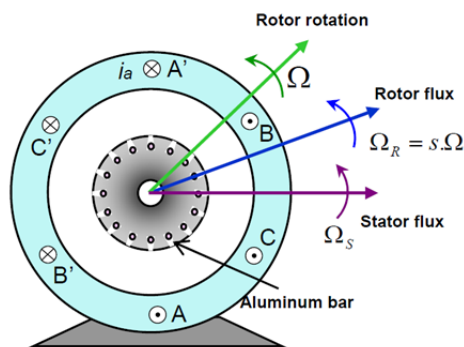


Figure 4: Squirrel cage rotor AC induction motor cutaway view

Stator rotating field speed (rad/s) :

$$\Omega_s = \frac{\omega_s}{p} \begin{cases} \omega_s : \text{AC supply freq (rad/s)} \\ p : \text{stator poles pairs number} \end{cases} \quad (1.1)$$

Rotor rotating speed (rad/s) :

$$\Omega = (1 - s)\Omega_s = (1 - s)\frac{\omega_s}{p} \quad (1.2)$$

1.4 MAGNETIC POWDER BRAKE

Magnetic powder brake (MPB) is a type of electromagnetic brake. When a DC voltage is applied to the MPB, a magnet powder is pasted around the rotor by the electromagnetic field. As a result, the MPB loads the motor. When the motor is loaded by MPB, very much heat is generated on the MPB. For this reason cooling is very important for MPB.

1.5 SENSORS FOR MOTOR CONTROL

Sensors, which are devices for measuring analog data, are used for the closed loop motor control. In the motor control system, we want to control the speed and torque. Torquemeter, which is a device for measuring the torque on a rotating system, is a kind of sensor. It is mounted between motor and load. An encoder is a sensor for measuring the speed. The basic encoder type, which is shown in Figure 5, consist of an optical encoder disk and a simple optocoupler. Optocoupler generate pulse signal when the optical encoder disk is rotated. If the period of the pulses is calculated, motor's speed value is found. But number of hole on the optical disk is very important for sensitivity and calculation.^{[25] [38]}

The speed calculation for a basic encoder is as follows:

$$\text{motor speed} = \frac{60}{T.n} \begin{cases} T: \text{period of pulse signal} \\ n : \text{number of holes} \end{cases} \quad (1.3)$$

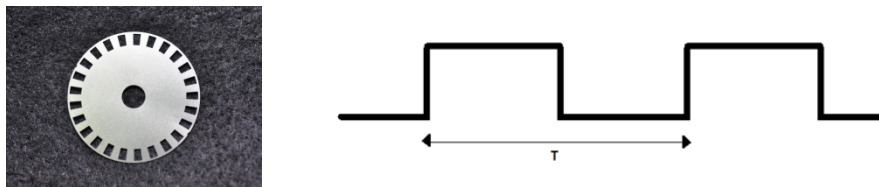


Figure 5: Encoder Disk and Output Signal

1.6 MOTIVATION AND PROBLEM DEFINITION

Nowadays training is very important for technical education. Educators want training sets for applying theoretical information in the real world such that student learn how to use the lecture material. For this reason training sets are made for learning the design of products which are commonly used in the market. Because of that, the three phase asynchronous AC induction motor driver is selected for this research. The motivation behind this research is to make an experiment platform for three phase asynchronous AC induction motor driver and deliver experience and understanding of the power electronic and control system design.

1.7 DESIGN REQUIREMENTS / CRITERIA

For this research, design requirements are divided into two parts, which are power electronics and system control. In the power electronics part, inverter and rectifier are designed. The inverter design requirements are as follows:

- Inverter should operate at least 1KW three phase asynchronous AC induction motor
- DC voltage input is minimum 400V/20A
- Switch input must be isolated for saving the microcontroller
- All generated signals can be observed by students

Rectifier parts design requirement are as follows:

- They must rectify single phase AC voltage
- They must rectify three phase AC voltage
- Outputs must be controlled for DC voltage amplitude
- All generated signals can be observed by students
- All designs must be modular

In system control part, microcontroller, torquemeter and encoder can be chosen. Microcontroller requirements are as follows:

- DSP-based microcontroller must be used in the research due to easy programming and user interface.

- Microcontroller must have at least six PWM outputs.
- Microcontroller must have at least two ADC inputs.
- Microcontroller must implement V/F control method
- Microcontroller must implement space vector modulation method

Torque meter requirements are as follows:

- Torque meter is able to measure 0-20Nm
- Torque meter is mounted between motor and load

Encoder requirements are as follows:

- Encoder consist of optical encoder disk and simple optocoupler
- Encoder must measure motor speed with enough sensitivity.
- Encoder output must be pulse signal.

CHAPTER II

IMPLEMENTATION

Modular design technique is used in this thesis. Code Composer Studio, which is a programming platform for Texas Instrument DSP, is used for coding the control algorithm. Eagle, which is a graphical layout editor, is used for PCB design. Matlab, which is a language of technical computing software, is used for finding the motor model and validation. D-LAB, which is a computer interface trainer, is used for data logging and computing. In this chapter, three-phase asynchronous AC induction motor driver design is described investigating each sub-block implementation. This research is divided into two main parts which are power electronic and system control. The power electronic part consists of inverter, rectifier and signal isolation sub-parts. The system control part consists of DSP controlcard and sensors (torquemeter and encoder). The main block diagram of the system is shown in Figure 6.

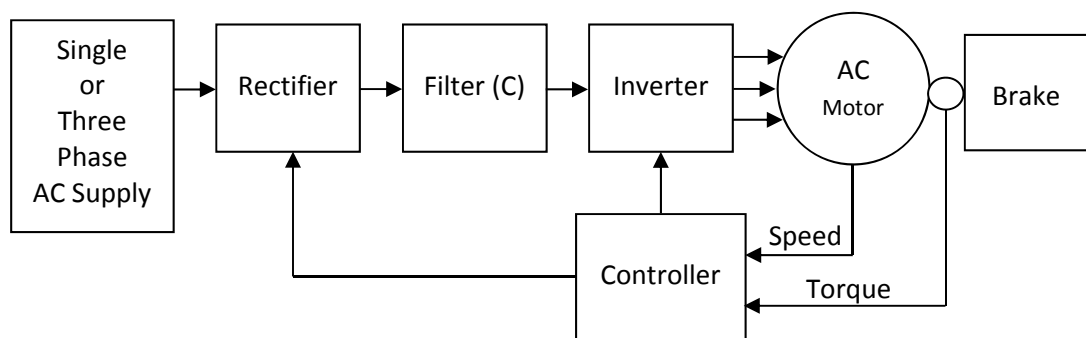


Figure 6: Main Block Diagram of the System

2.1 POWER ELECTRONIC MODULE DESIGN

2.1.1. Rectifier Design

Four kind of rectifiers are designed in this thesis. They are uncontrollable single phase rectifier, controllable single phase rectifier, uncontrollable three phase rectifier, controllable three phase rectifier. All rectifier types are designed in a modular way.

Diodes, which are two terminal electronic components with low resistance to current flow in one direction and high resistance in the other direction, are used for uncontrollable single or three phase rectifier design. One module is designed which consists of six diodes. Each diode is independent on the module. Hence, it is possible that the single-phase rectifier uses 4 diodes and the three-phase rectifier uses 6 diodes on the module. IOR 25F120, which is a standard recovery diode, is used. Voltage and current maximum ratings are 1200V/25A. Diode voltage and current values suitable for the design in the thesis. A schematic of the diode module is shown in Figure 7.^[26]

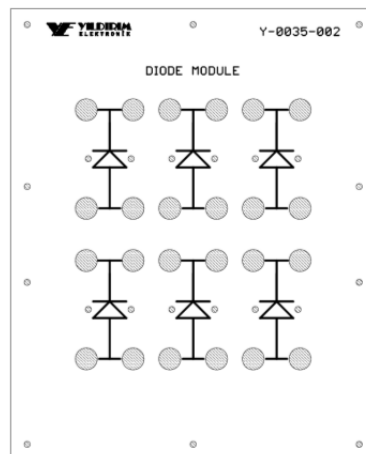


Figure 7: Diode Module Design

We use thyristors for the controlled single or three phase rectifier designs. A thyristor is a solid-state semiconductor device with four layers of N and P type material. Thyristor conducts when its gate receives a current trigger and continues to conduct while it is forward biased. Three modules are designed for the single and three phase rectifier. They are thyristor module, single phase thyristor controller

module, three phase thyristor controller module. The thyristor module is used in both thyristor controller modules and consists of six thyristors. Each thyristor is independent. Hence, it is possible that the single phase rectifier uses 4 thyristors and the three phase rectifier uses 6 thyristors on the module. IOR 25RIA120, which is a medium power thyristor, is used for each diode. Voltage and current maximum ratings are 1200V/25A. Thyristor voltage and current values are chosen to fit the requirements in the thesis. A schematic of the thyristor module is shown in Figure 8. [26]

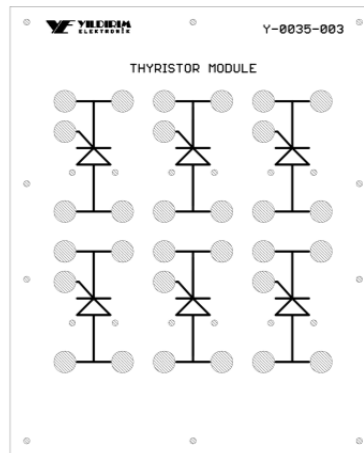


Figure 8: Thyristor Module Design

Single-phase thyristor controller module is used to realize the controllable single-phase rectifier. It generates 4 trigger signals for the thyristors. When the AC input signal is positive, first and third outputs generate the trigger signal. Otherwise the AC input signal is negative, and the second and fourth outputs generate the trigger signal. If the thyristor trigger time is controlled in the AC input voltage's period by single phase thyristor controller, the DC voltage output amplitude is controlled. The rectified voltage for the thyristor control method is shown in Figure 9. In this module design, TCA785, which is a phase control integrated circuit (IC), is used. This phase control IC is intended to control thyristors, triacs and transistors. In addition, CD4050, which is a buffer, duplicates the output of the TCA785. BD139, which is a NPN transistor, drives the output signals. Transformers are used for isolating the module outputs. Single phase thyristor controller module design is shown in Figure 10. [26]

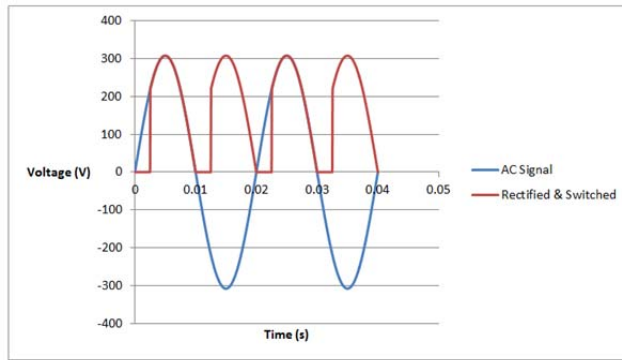


Figure 9: Single Phase Rectifier DC Voltage Output with Thyristors

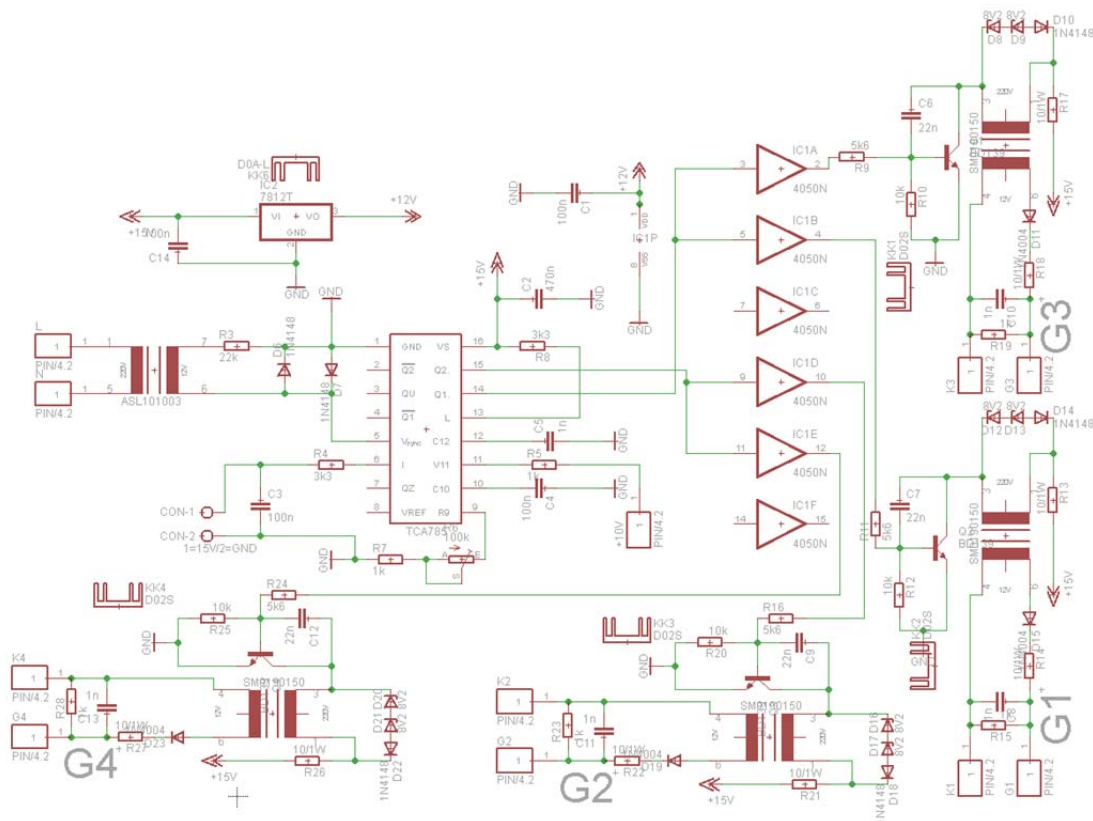


Figure 10: Single Phase Thyristor Controller Design

Three phase thyristor controller module, which is shown in Figure 12, is used for controllable three phase rectifier. It generates 6 trigger signals for the thyristors. When the three phase AC input signal is positive, the first output of each phase generates the trigger signal. Otherwise if the three phase AC input signal is negative, each second output generates trigger signal. Together, control of the thyristor trigger time allows to control the DC voltage output amplitude. For this

method, the DC voltage output is shown in Figure 11. In principle, this module design is identical to the single phase thyristor controller module. Only three TCA785 are used in the design and generate two trigger outputs for each AC voltage phase. As a result, the three phase thyristor control module can trigger six thyristors.^[26]

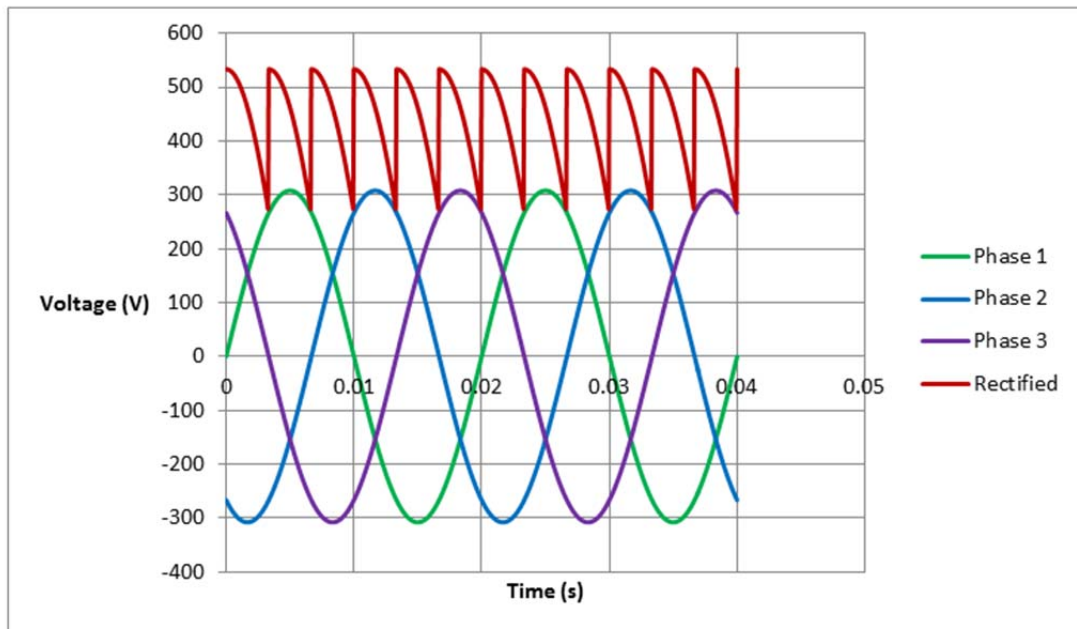


Figure 11: Three Phase Rectifier DC Voltage Output with Thyristors

2.1.2. Inverter Design

The inverter, which is an electrical device that changes DC voltage to AC voltage, is designed using transistors. Here, the kind of transistor is very important for the design. In this thesis, IGBTs are used in the design, because they come with the advantage of high current handling capability of bipolar transistors with the ease of control of a MOSFET transistor. The application area of IGBTs and MOSFETs is illustrated in Figure 13. IGBTs are preferred under the following conditions:

- Low duty cycle
- Low frequency (<20kHz)
- High voltage application
- Operation at high junction temperature is allowed (>100°C)

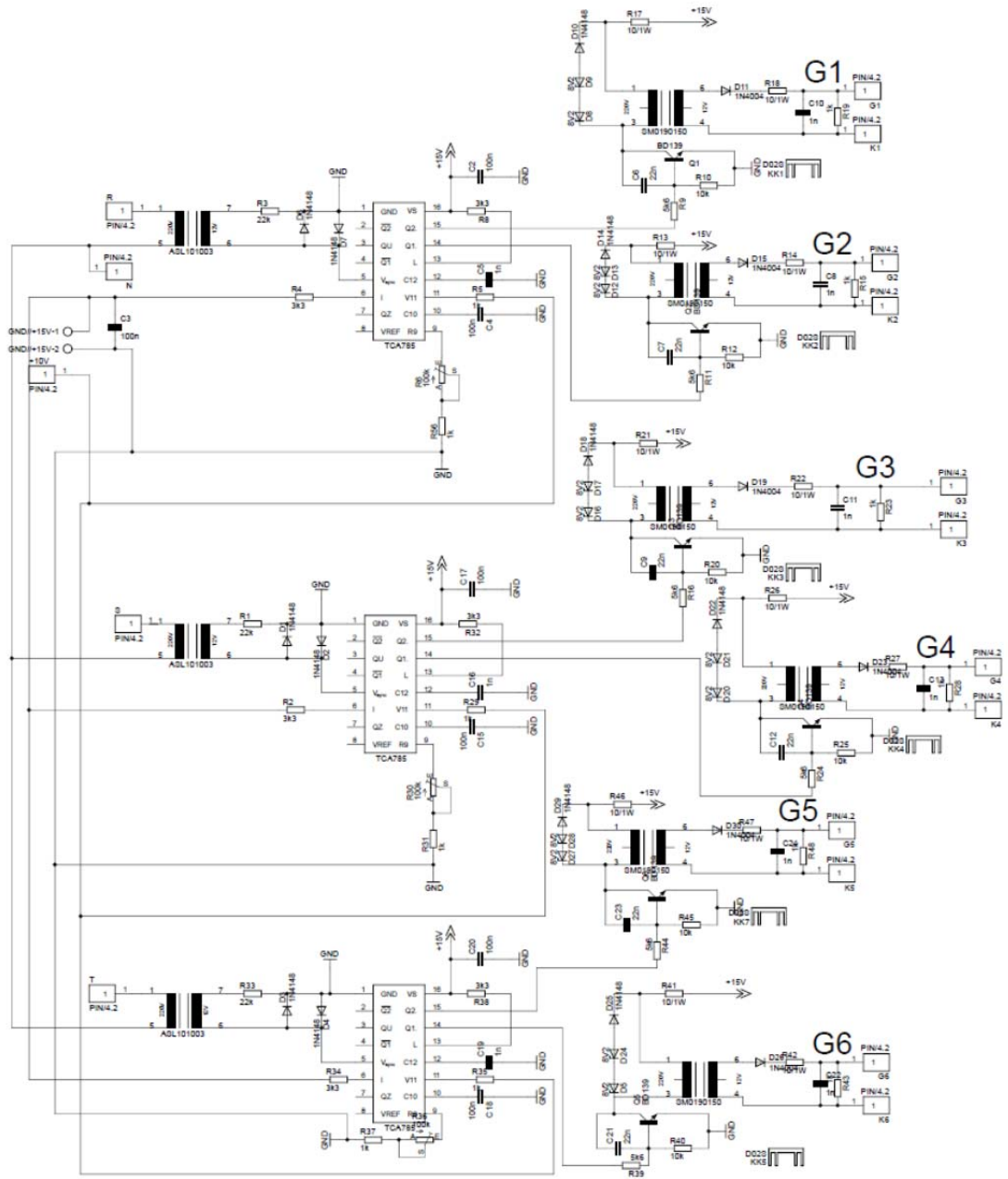


Figure 12: Three Phase Thyristor Controller Module

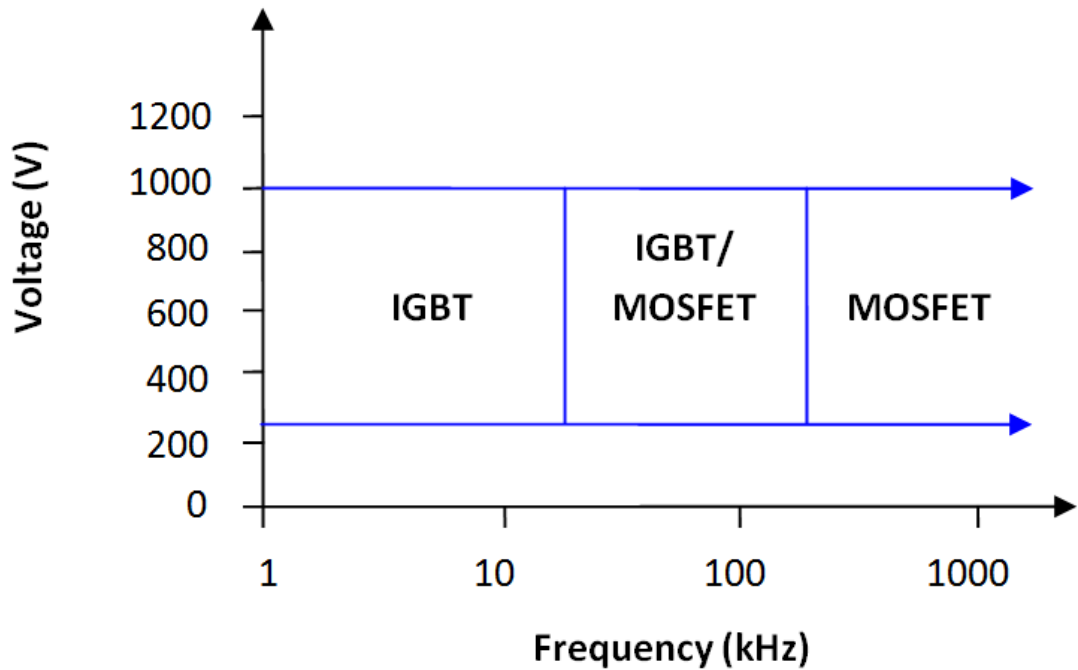


Figure 13: Where MOSFETs and IGBTs are preferred

For this reason, 7MBP50RJ120, which is an IGBT block, is used in the inverter design. This block consists of 7 IGBTs. Voltage and current maximum ratings are 1200V/50A. This block needs four isolated DC power supplies (+15V) for operating properly. Each up-side IGBT has an own isolated DC power supply. The down-side three IGBTs are supplied by one isolated DC supply. Each up-side IGBT has an own alarm output, whereas the down-side three IGBTs use the same alarm output. When each alarm output is active, the IGBT block stops to run. 7MBP50RJ120 block diagram is shown in Figure 14.^{[26] [12] [17] [10]}

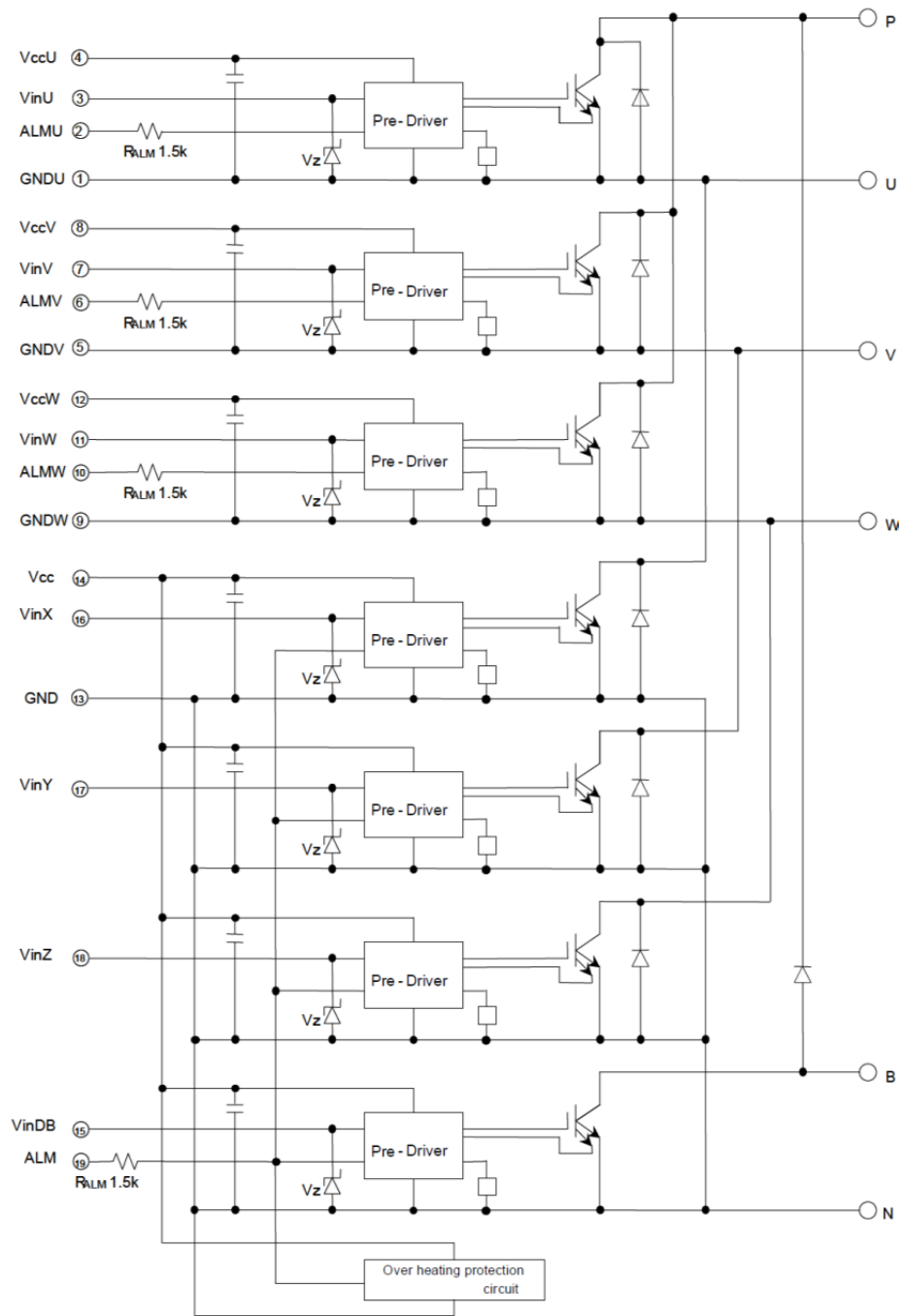


Figure 14: Block Diagram of 7MBP50RJ120 ^[17]

In this thesis, one +15V DC power supply is used for the inverter realization. The other four isolated DC supplies are generated by the DC-DC converter (SPR01M15). The isolated four DC supply design is shown in Figure 15.

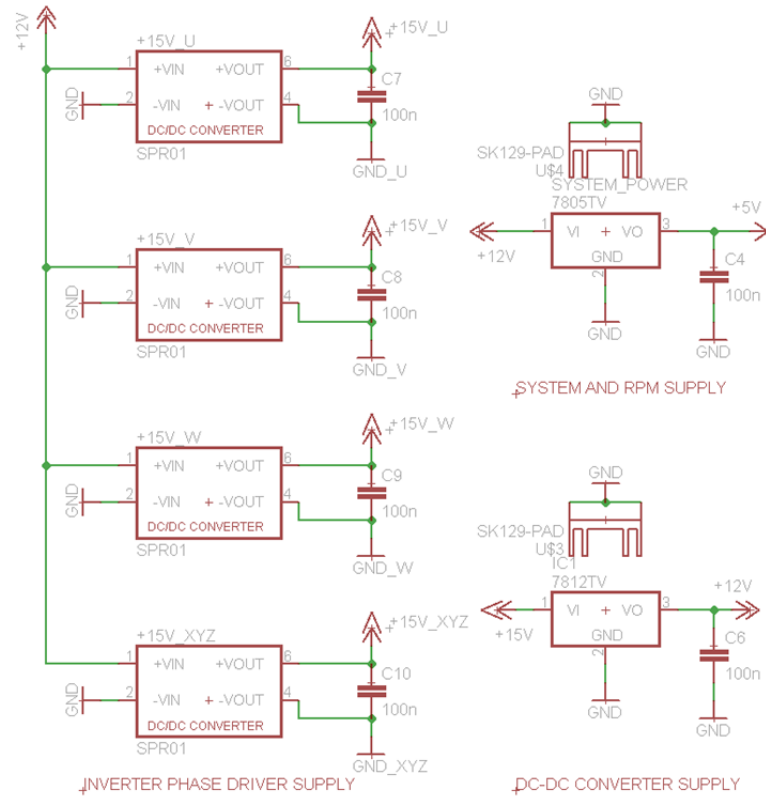


Figure 15: Isolated Four DC Supply Design

Isolation is very important for the inverter design. The IGBT block needs four isolated DC power supplies for running. As a result, the microcontroller and IGBTs gate inputs have different ground levels. For this reason the microcontroller PWM outputs can not be directly connect to the IGBTs gate inputs, since isolation must be provided. Also microcontroller PWM outputs must be isolated for saving. Since the PWM outputs are digital signals. An optocoupler is enough for isolating the PWM outputs. In this thesis, HCPL4502, which is high speed transistor optocoupler, is used for isolating microcontroller PWM outputs. PWM outputs isolation design is shown in Figure 16.

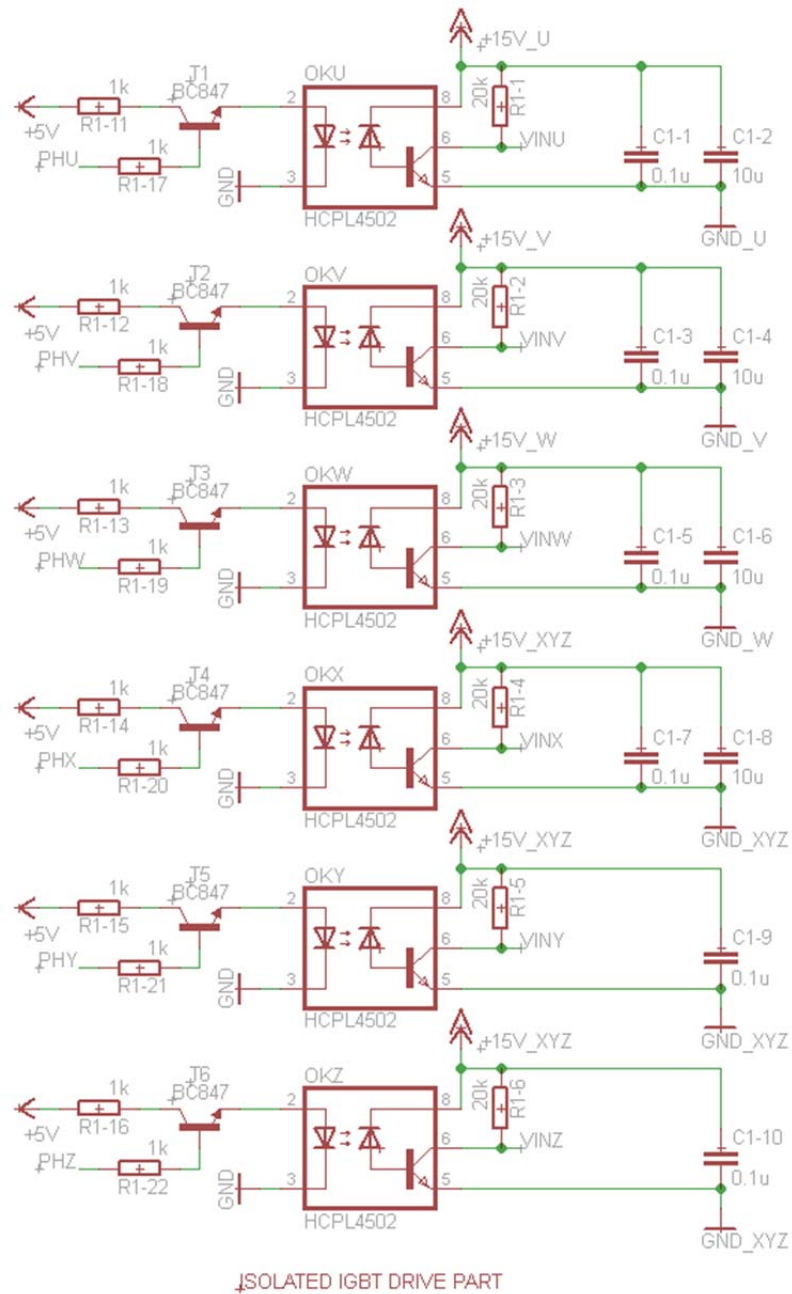


Figure 16: Isolated IGBT Drive Part

Alarm outputs must be connected to the microcontroller digital inputs for warning. But IGBT block and microcontroller's ground level is not same. Hence, isolated alarm outputs are generated for protecting the microcontroller. Isolated alarm outputs are shown in Figure 17.

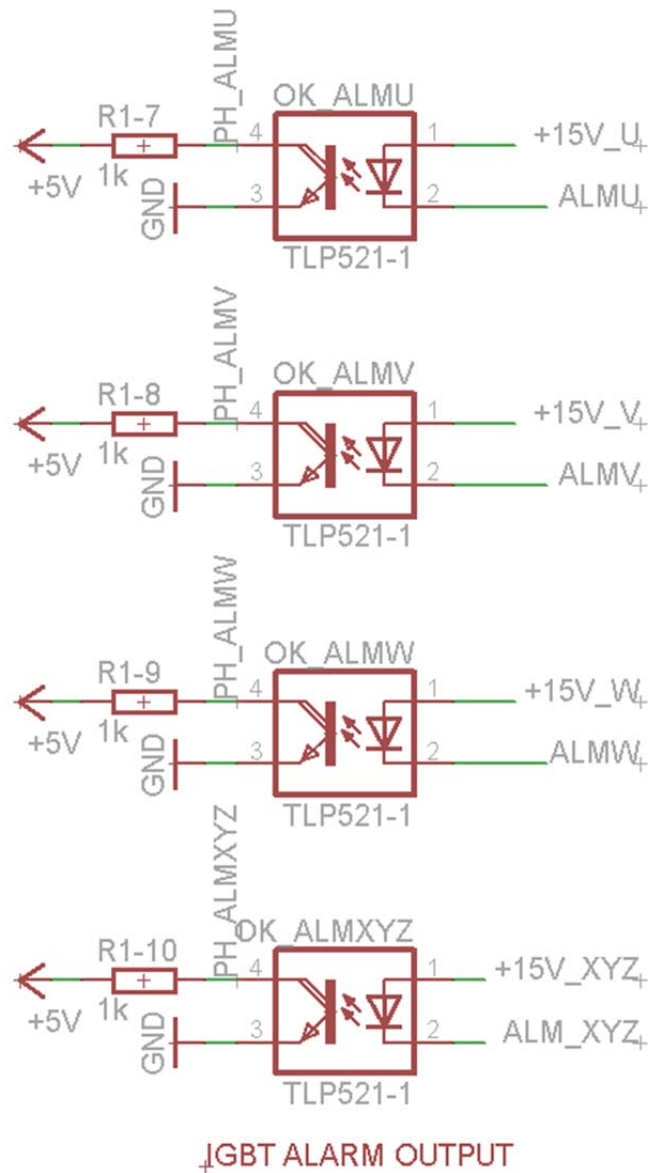


Figure 17: Isolated IGBTs Alarm Output Design

In this thesis, the torque meter and encoder device are connected to the inverter card in order to achieve a compact design. Their output signals are carried over to the microcontroller interface connector. Hence, the inverter card is only a carrier for torque meter and encoder outputs. Inverter card is shown in Figure 18.

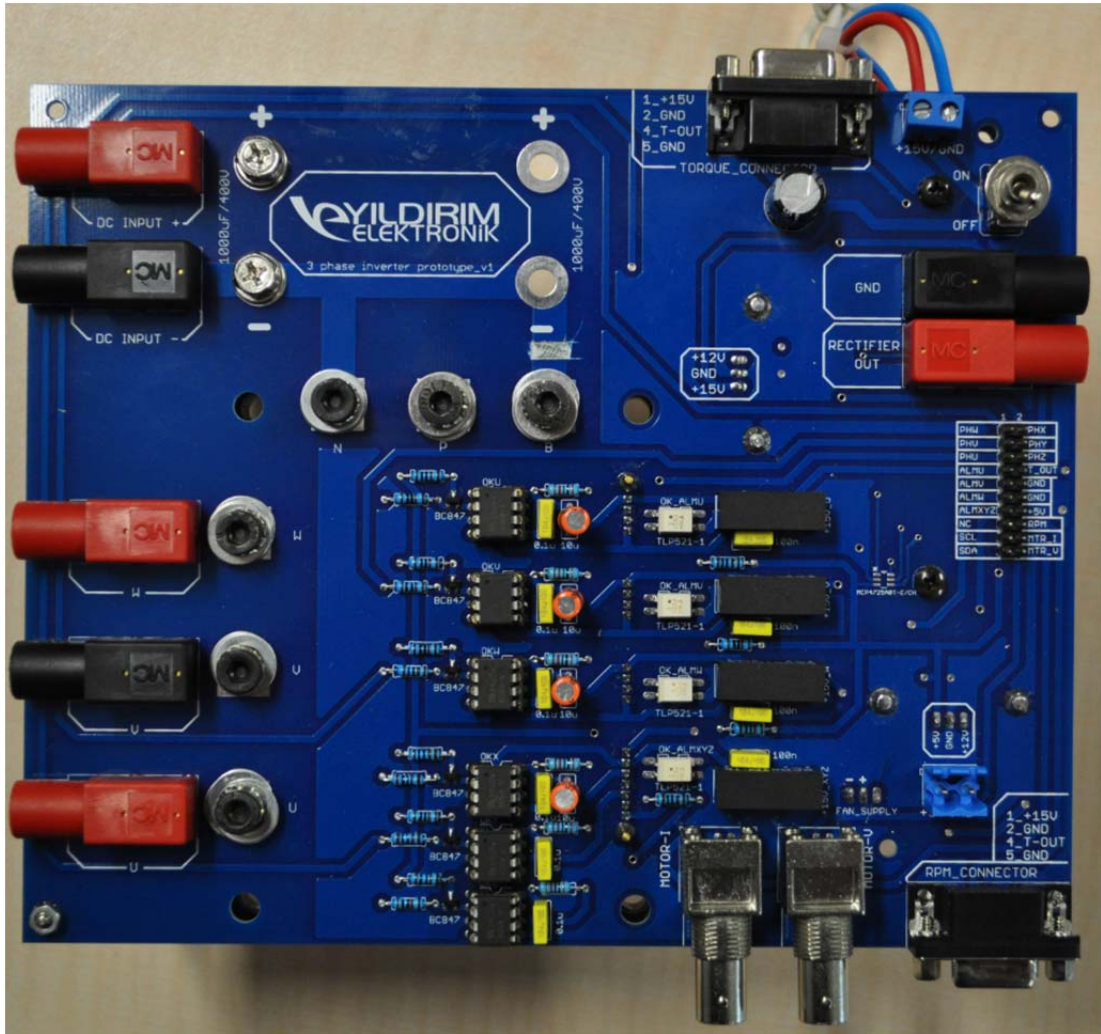


Figure 18: Inverter Card

2.2 SYSTEM CONTROL MODULE DESIGN

2.2.1. Scalar Control

In this thesis, the scalar control (V/F) method is used. It performs speed control of induction motor by the adjustable magnitude of stator voltages and frequency in such a way that the air gap flux is always maintained at the desired value at the steady-state. The working principle of this method is shown in Figure 19, in a simplified version of the steady-state equivalent circuit. Hence, the stator resistance (R_s) is assumed to be zero, the stator leakage inductance (L_{ls}) is embedded into the rotor leakage inductance (L_{lr}) and the magnetizing inductance is moved in front of the total leakage inductance ($L_l = L_{ls} + L_{lr}$). The phasor equation of the magnetizing

current (generates the air gap flux) for steady-state analysis is given in equation 2.1 which is approximately the stator voltage to frequency ratio.^[2]

$$\tilde{I}_m \cong \frac{\tilde{V}_s}{j\omega L_m} \quad (2.1)$$

If the AC induction motor is operating in the linear magnetic region, L_m is constant. So that equation 2.1 can be shown in terms of magnitude as;

$$I_m = \frac{\Lambda_m}{L_M} \cong \frac{V_s}{(2\pi f)L_m} \Rightarrow \Lambda_m \propto \frac{V_s}{f} \quad (2.2)$$

Where V and Λ represent the magnitude of stator voltage and stator flux, and \tilde{V} represents the phasor.

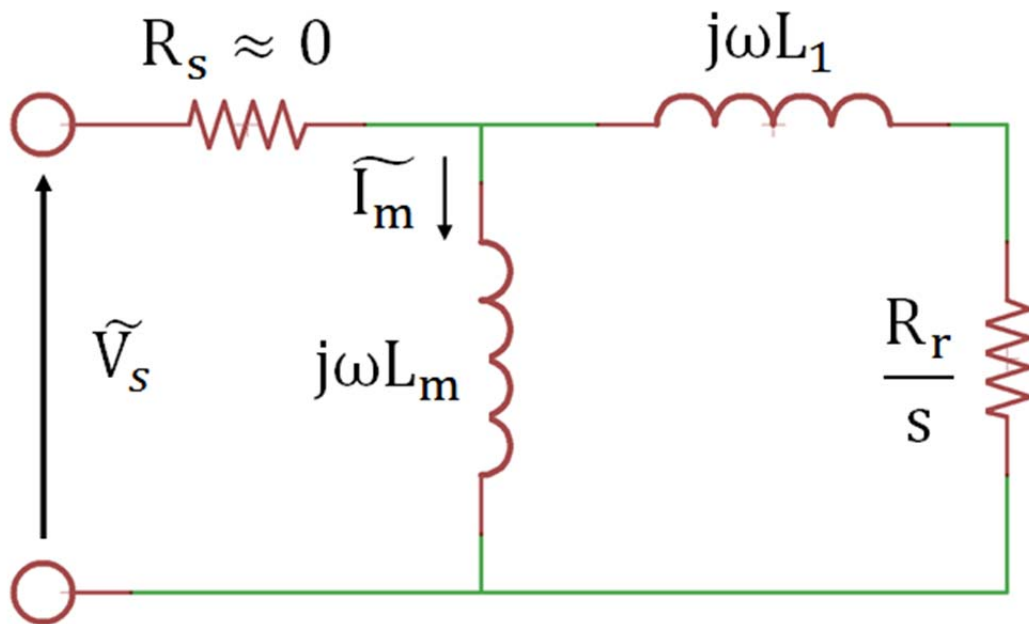


Figure 19: Simplified steady-state equivalent circuit of induction motor

As seen in Equation 2.2, if the ratio V/f is constant for any frequency, the flux is constant and the torque becomes independent from the power supply frequency. In order to keep the flux Λ_m constant, the ratio of V_s/f must be constant at a different speed. If the motor speed increases, the stator voltage must also be increased in order to keep the constant ratio of V_s/f . But due to a slip as a function of the motor load, the frequency is not equal to the real speed. If there is no load which means

slip is very small, the motor speed is almost equal to the synchronous speed. In this case, the open loop V/F system will realized the desired speed. However, The V/F system is not be able to control the speed precisely if an load is applied. If the speed is measured within the system, the slip compensation can simply be included. The closed loop V/F system is shown below in Figure 20.^[47]

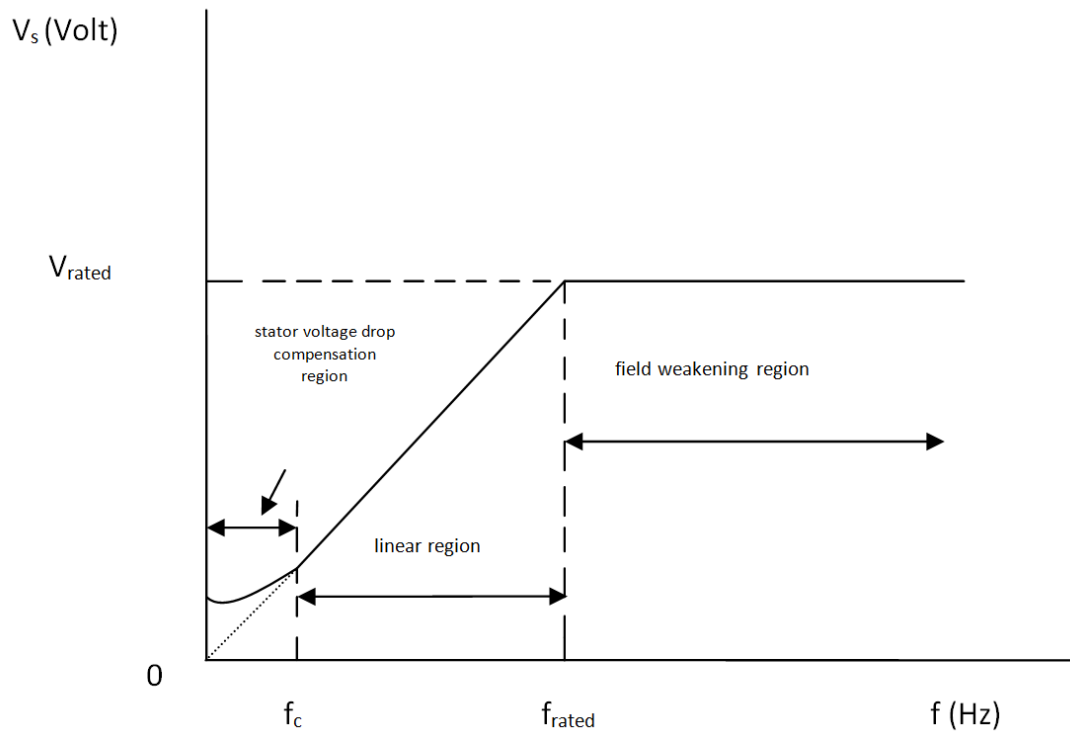


Figure 20: Stator Voltage vs Frequency Profile under V/F control

Usually, the V/F ratio is based on the rated values of these variables. The three speed ranges in the V/F profile are listed below:

- At $0-f_c$, V/F profile is not linear since the voltage drop across the stator resistance can not be neglected and must be compensated for by increasing V_s . It is possible to compute the cutoff frequency (f_c) and the suitable stator voltages analytically from the steady-state equivalent circuit with $R_s \neq 0$.
- At f_c-f_{rated} , this region V/F is linear. Flux (V/F) is constant at this region.
- It is not possible to keep V/F constant at higher frequencies than f_{rated} since the stator voltages would be limited at the rated value in order to avoid any insulation breakdown at the stator windings. For this reason, the air gap flux would be reduced which decreases the torque.

If the stator flux is constant, the torque depends only on the slip speed as shown in Figure 21. The torque and speed of an AC induction motor is able to be controlled with the constant V/F , by regulating the slip speed.^{[47] [2]}

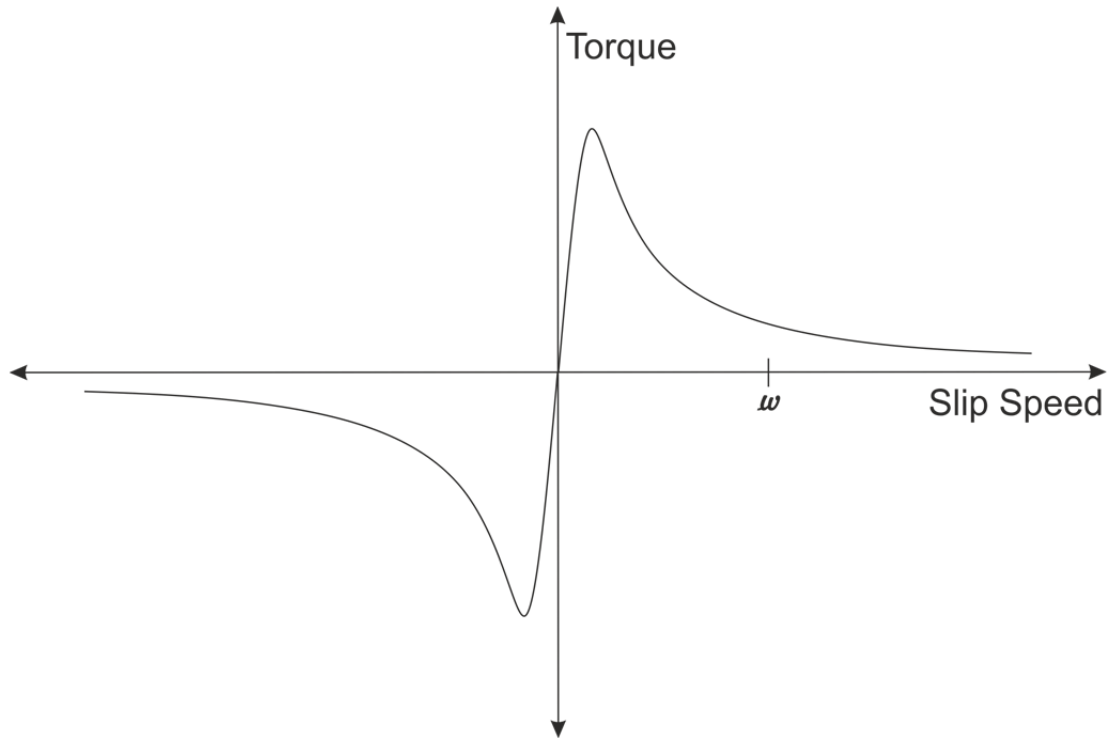


Figure 21: Torque vs Slip Speed of an Induction motor with Constant Stator Flux

In this thesis, cutoff frequency (f_c) is selected to 24Hz and f_{rated} is selected to 60Hz. V_{rated} is a maximum single phase full rectified signal, which is 285VDC. Hence, all experiments are made in the linear region.

2.2.2. Space Vector Modulation Method

Space vector modulation method (SPVM) is used for generating PWM signals which control the inverter gate inputs. The structure of the typical three phase voltage source inverter (VSI) is shown in Figure 22. V_a , V_b and V_c are the output voltages of the inverter. Q1-Q6 are power transistors which are controlled by gate inputs (a , a' , b , b' , c , c'). When each upper transistor is switched on, the corresponding lower transistor is switched off. The state of gate inputs (a,b,c) are sufficient to evaluate the output voltage.^{[48] [30]}

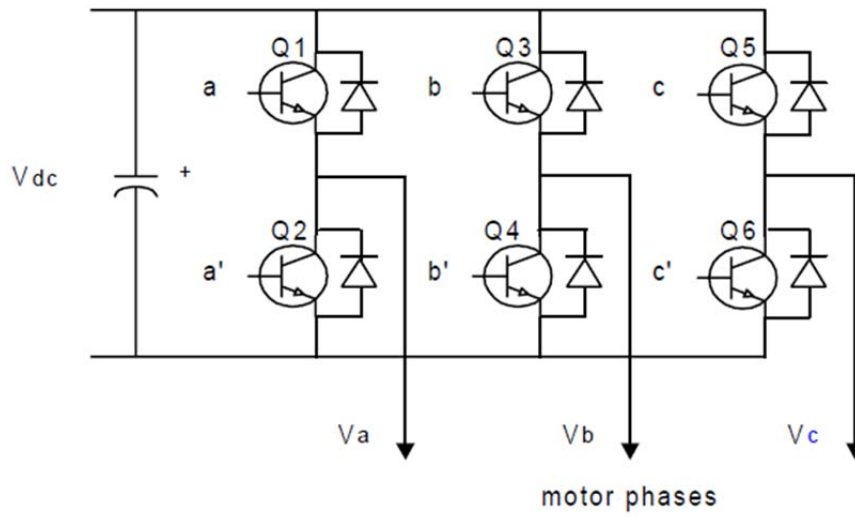


Figure 22: Typical Three Phase VSI Diagram

The relationship between the switching variable vector $[a \ b \ c]t$, the line-to-line output voltage vector $[V_{ab} \ V_{bc} \ V_{ca}]t$ and line-to-neutral output voltage vector $[V_a \ V_b \ V_c]t$ are shown in equations 2.3 and 2.4 where V_{dc} refers to the DC supply voltage.^{[35] [46]}

$$\begin{bmatrix} V_{ab} \\ V_{bc} \\ V_{ca} \end{bmatrix} = V_{dc} \begin{bmatrix} 1 & -1 & 0 \\ 0 & 1 & -1 \\ -1 & 0 & 1 \end{bmatrix} \begin{bmatrix} a \\ b \\ c \end{bmatrix} \quad (2.3)$$

$$\begin{bmatrix} V_a \\ V_b \\ V_c \end{bmatrix} = \frac{1}{3} V_{dc} \begin{bmatrix} 2 & -1 & -1 \\ -1 & 2 & -1 \\ -1 & -1 & 2 \end{bmatrix} \begin{bmatrix} a \\ b \\ c \end{bmatrix} \quad (2.4)$$

The derived output line-to-line and phase voltages in terms of DC supply voltage V_{dc} for the eight possible combinations of on and off states for the three upper power transistors of typical three phase VSI are given in table 1^{[37] [18]}

a	b	c	V_a	V_b	V_c	V_{ab}	V_{bc}	V_{ca}
0	0	0	0	0	0	0	0	0
1	0	0	2/3	-1/3	-1/3	1	0	-1
1	1	0	1/3	1/3	-2/3	0	1	-1
0	1	0	-1/3	2/3	-1/3	-1	1	0
0	1	1	-2/3	1/3	1/3	-1	0	1
0	0	1	-1/3	-1/3	2/3	0	-1	1
1	0	1	1/3	-2/3	1/3	1	-1	0
1	1	1	0	0	0	0	0	0

Table 1: Device ON/OFF State and Corresponding Outputs of Three Phase VSI

If it is assumed that d and q are the fixed horizontal and vertical axes in the plane of the three motor phases, the vector representations of the phase voltages corresponding to the eight combinations can be obtained by applying the d-q transformation to the phase voltages:

$$T_{abc-dq} = \sqrt{\frac{2}{3}} \begin{bmatrix} 1 & -\frac{1}{2} & -\frac{1}{2} \\ 0 & \frac{\sqrt{3}}{2} & -\frac{\sqrt{3}}{2} \end{bmatrix} \quad (2.5)$$

The transformation is equivalent to an orthogonal projection of [a, b, c]^t onto the two dimensional plane perpendicular to the vector [1, 1, 1]^t in a three-dimensional coordinate system, the results of six non-zero vectors and two zero vectors are shown in Figure 23. The nonzero vectors form the axes of a hexagonal and the angle between any adjacent two non-zero vectors is 60 degrees. The zero vectors are at the origin and apply zero voltage to a three-phase load. The eight vectors are called the Basic Space Vectors and are referred to as U₀, U₆₀, U₁₂₀, U₁₈₀, U₂₄₀, U₃₀₀, O₀₀₀ and O₁₁₁.^{[18] [37] [46]}

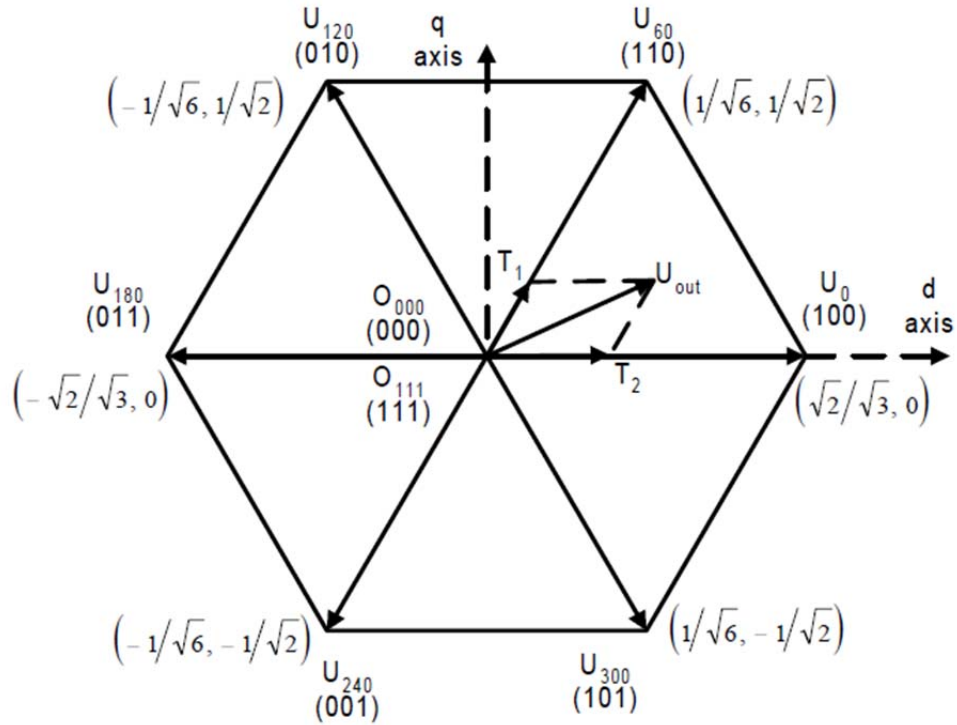


Figure 23: The Basic Vectors and Switching States

As the d-q transform is applied to a desired three-phase voltage output, a desired reference voltage vector U_{out} is being obtained in the d-q plane as shown in Figure 23. The magnitude of U_{out} is the RMS value of the corresponding line-to-line voltage with the defined d-q transform.

By the combination of the switching states that are corresponding to the basic space vectors, the reference voltage U_{out} is approximated. The average inverter output is the same as the average reference voltage U_{out} for any small period of time (T), as shown in equation 2.6. T_1 and T_2 are respective durations for switching states corresponding to U_x and U_{x+60} (or U_{x-60}) are applied.

U_x and U_{x+60} are the basic space vectors, and U_{out} consists of U_x and U_{x+60} . But if the reference voltage U_{out} is changed even a bit within T , the equation 2.6 becomes equation 2.7, in which $T_1 + T_2 \leq T$. It is very important that T is very small in respect to the speed change of U_{out} .^{[35] [48] [30]}

$$\frac{1}{T} \int_{nT}^{(n+1)T} U_{out}(t) dt = \frac{1}{T} (T_1 U_x + T_2 U_{x\mp 60}) \quad (2.6)$$

$$U_{out}(nT) = \frac{1}{T} (T_1 U_x + T_2 U_{x\mp 60}) \quad (2.7)$$

The sum of T1 and T2 must be less than or equal to T_{pwm}. The inverter needs to be in zero state for the rest of period. For T1 + T2 + T0 = T_{PWM} = T, equation 2.7 becomes equation 2.8.

$$T_{PWM} U_{out} = T_1 U_x + T_2 U_{x\pm 60} + T_0 (O_{000} \text{ or } O_{111}) \quad (2.8)$$

Equation 2.8 is used for calculating the equation 2.9

$$[T_1 \ T_2]^t = T_{PWM} [U_x \ U_{x\pm 60}]^{-1} U_{out} \quad (2.9)$$

where $[U_x \ U_{x\pm 60}]^{-1}$ is normalized decomposition matrix for sector.

In order to calculate T1 and T2, we may assume the angle between U_{out} and U_x is α . Accordingly, the T1 and T2 equations are shown in equation 2.10.

$$\begin{aligned} T_1 &= \sqrt{2} T_{PWM} |U_{out}| \cos(\alpha + 30^\circ) \\ T_2 &= \sqrt{2} T_{PWM} |U_{out}| \sin(\alpha) \end{aligned} \quad (2.10)$$

2.2.3. Control System Design

Texas Instruments TMS320F28035 Piccolo DSP is used in this research. It is special microcontroller for motor control due to the easy implementation capability of V/F control and space vector modulation PWM method. It is very capable for future upgrading. It's highlighted features are explained in:^{[28] [39] [41]}

- High-Efficiency 32-bit CPU
- 60MHz device
- Single 3.3V supply
- Integrated power-on and brown-out resets
- Two internal zero-pin oscillators
- Up to 45 multiplexed GPIO pins

- Three 32-bit timers
- On-chip flash, SARAM, OTP Memory
- Serial port peripherals (SCI/SPI/I2C/LIN/eCAN)
- Enhanced control peripherals
 - Enhanced Pulse Width Modulator (ePWM)
 - High-Resolution PWM (HRPWM)
 - Enhanced Capture (eCAP)
 - High-Resolution Input Capture (HRCAP)
 - Enhanced Quadrature Encoder Pulse (eQEP)
 - Analog to Digital Converter (ADC)
 - Comparator

The control system is designed as both open loop and closed loop systems. For open loop control, V/F and SVGEN program functions are used. Motor speed is adjustable by the speed reference which is given by the end user. If the motor is loaded, the system may not keep the speed at the desired value. The open loop system that is developed for this research is shown in Figure 24.

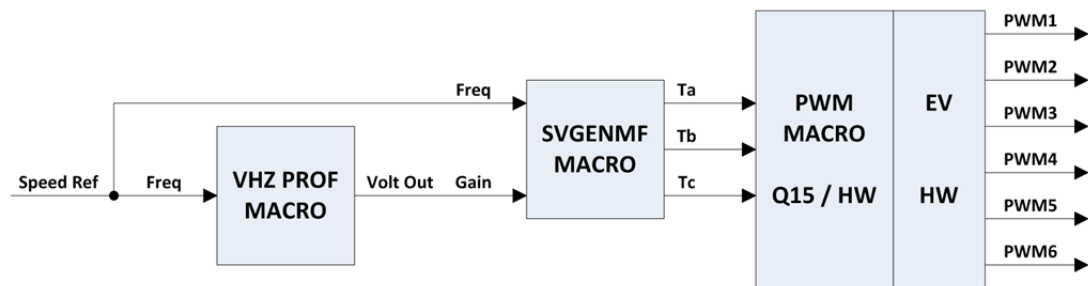


Figure 24: V/F controlled Open Loop System

Firstly open loop system is operated and later encoder is mounted to the system for measuring the speed. F28035 DSP's CAP input pin is used for measuring the speed by the use of pulse signal that is generated by encoder. With the help of the CAP program function, the period of the pulse signal is measured. The multiplication of the period data (T) and the number of slots on the encoder disk (n) gives the RPM value (nT). The block diagram of this structure is given in Figure 25.

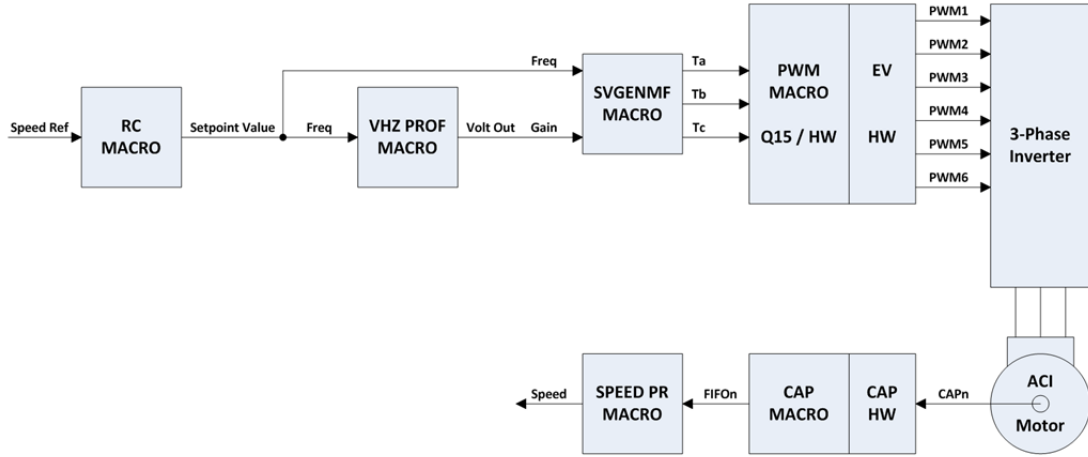


Figure 25: V/F controlled Open Loop system with speed measurement

When the motor is loaded, the system does not keep the speed at the desired level. So closed loop control is necessary for keeping the speed for the different load levels. It is adequate to measure speed value in a closed loop system in order to keep the speed value at the desired level. Equation 2.11 is used to form the closed loop system. As it is shown in equation 2.12, the PID control algorithm is applied to the error signal. So the system plant of this research is formed as it is shown in equation 2.13. V/F controlled closed loop system is shown in Figure 26.

$$e(s) = SP - PV \begin{cases} SP: \text{Set point (speed or torque reference)} \\ PV: \text{Process variable (measured speed or torque)} \\ e(s): \text{Error} \end{cases} \quad (2.11)$$

$$u(t) = K_p e(t) + K_i \int_0^t e(t) dt + K_d \frac{d}{dt} e(t) \quad (2.12)$$

$$PI = SP + u(t) \quad \{PI: \text{Plant Input}\} \quad (2.13)$$

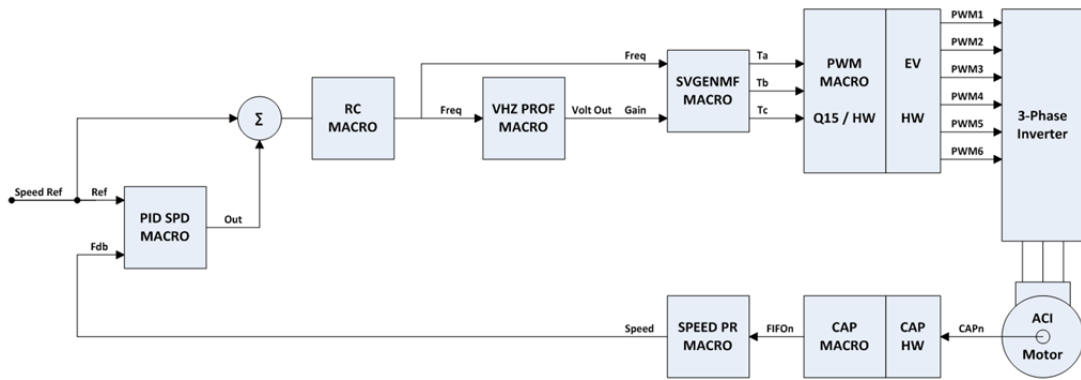


Figure 26: V/F Controlled Closed Loop System with Speed Sensor

Although the previous paragraphs are only explaining the constant speed control, torque is the other control parameter of this system. In V/F method, maximum torque is applied to the AC motor. If maximum torque is not necessary for the system, it is waste of power. So that in this research power efficiency is increased by controlling the DC supply voltage value. The critical torque value, which stops the motor operation, should be known for each load value. In this research, critical torque values are measured for loads and a look-up table is generated. For the control of maximum torque level, the instant torque value is measured by the torquemeter which is the sufficient level for the present condition. Then the DC supply voltage level is decided according to the look up table and the F28035 DSP controls the rectifier part for generating this DC supply voltage. So that the required torque is generated by AC motor. The block diagram of this system part is shown in Figure 27.

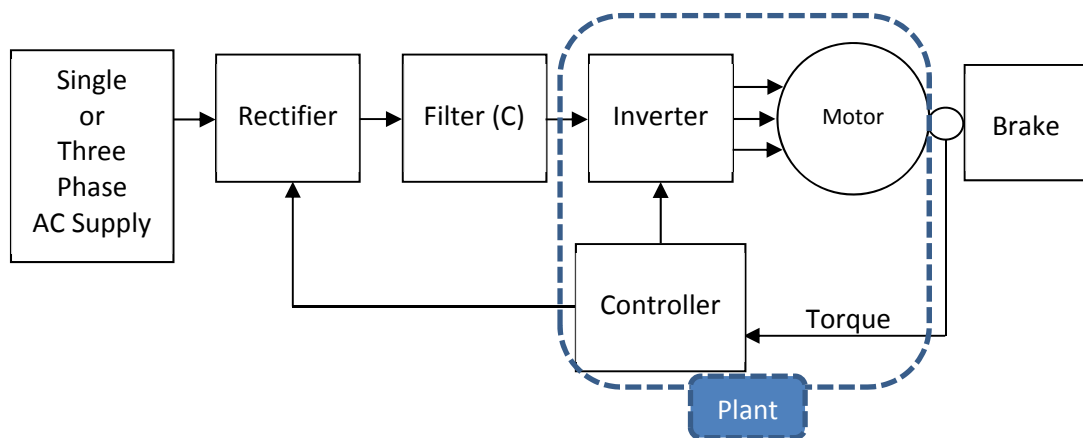
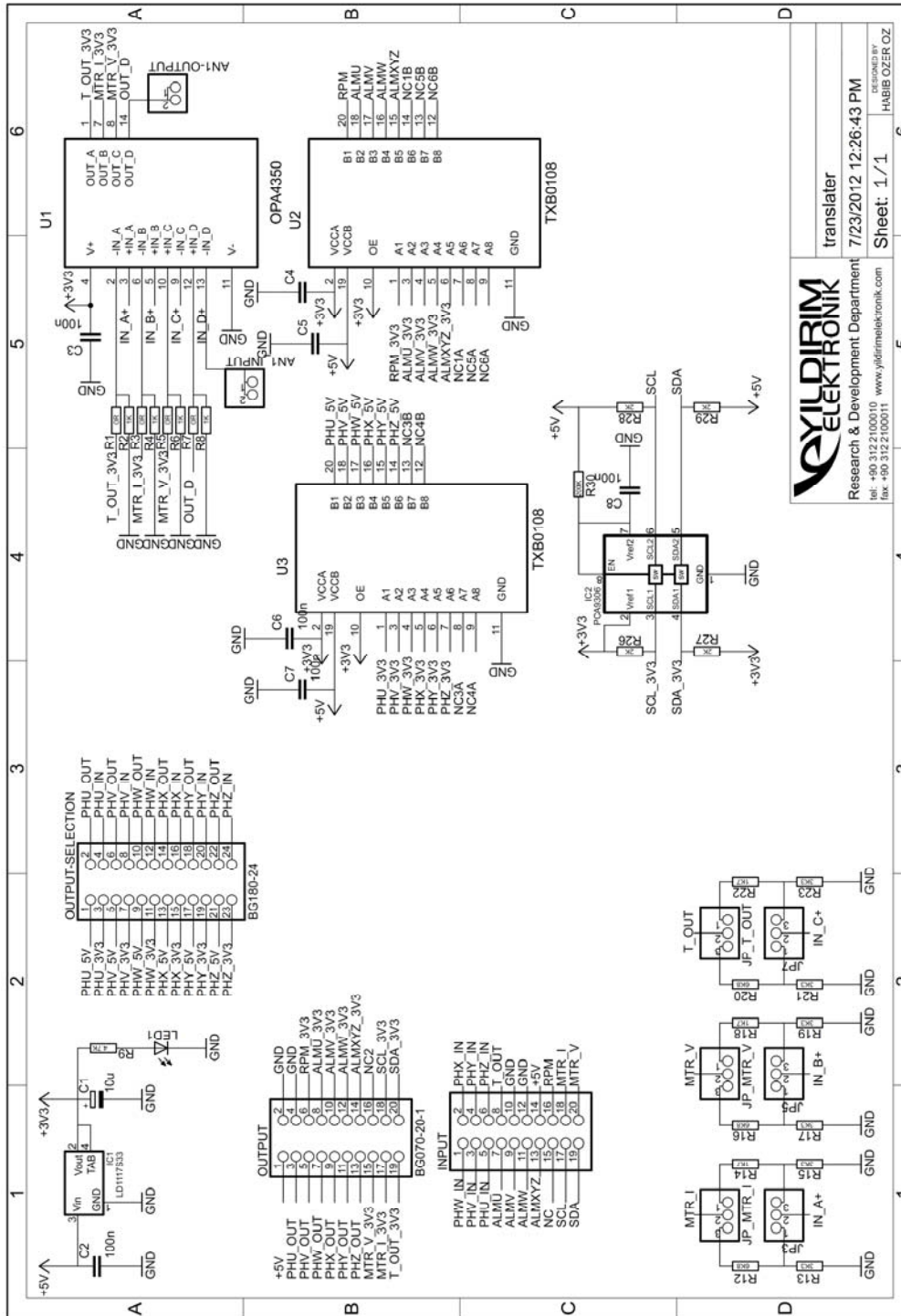


Figure 27: DC Supply Input Control for Closed Loop Torque Control

2.3 INTEGRATION

The overall system in this thesis consists of many subsystems that should be integrated carefully. The first problem of integration concerns the ground levels which should be common except for the isolated circuitry's ground levels. For this reason the inverter, rectifier and microcontroller subsystem grounds are connected to each other. The second problem of integration is the isolation requirement of the AC voltage input with the mains for safety and measurement reliability. Since the high end bench top measurement devices such as oscilloscopes are usually capable of measurements with respect to the mains ground level, it is convenient to use a differential probe for isolated subsystems of this study. The third problem of integration is the requirement of an analog voltage output for controlling the rectifier subsystem. Since the F28035 DSP does not include a digital to analog converter (DAC), an external DAC integrated circuit (IC) is used on the inverter printed circuit board (PCB) for the rectifier control. The fourth problem of integration is about different supply voltage levels which affects the communication between subsystems due to the difference in digital input/output (I/O) high and low levels. Since the F28035 DSP supply is 3.3V while the rest of system, including encoder and inverter, is operating with 5V; the bidirectional voltage level translator TXB0108 is used for digital I/O. Also, since the MCP4725 of inverter subsystem uses inter-integrated circuit (I2C) bus for the interface, the bidirectional I2C bus voltage level translator PCA9306 is used. Another problem is that F28035 DSP's analog to digital converter (ADC) input voltage level is between 0-3.3V while the torquemeter output voltage level is between 0-5V. Hence, OPA4350, which is a high speed operational amplifier, is used for decreasing the voltage level of the ADC input. A PCB card is designed for F28035 prescaling integration problems. The schematic design is shown in Figure 28 and PCB design is shown in Figure 29.



YILDIZIM ELEKTRONIK
 Research & Development Department
 7/23/2012 12:26:43 PM
 DESIGNED BY
 HABIB OZER OZ
 Sheet: 1 / 1

Figure 28: Translator Card Schematic Design

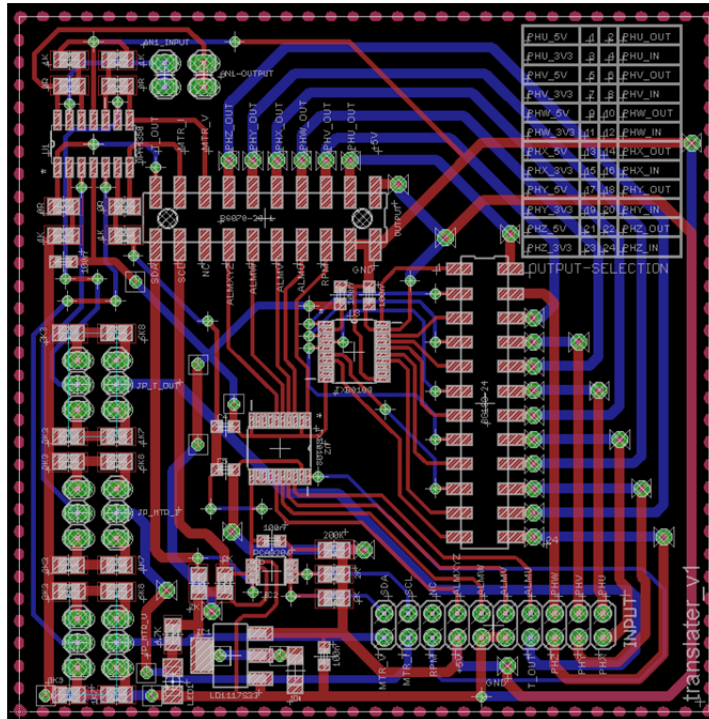


Figure 29: Translator Card PCB Design

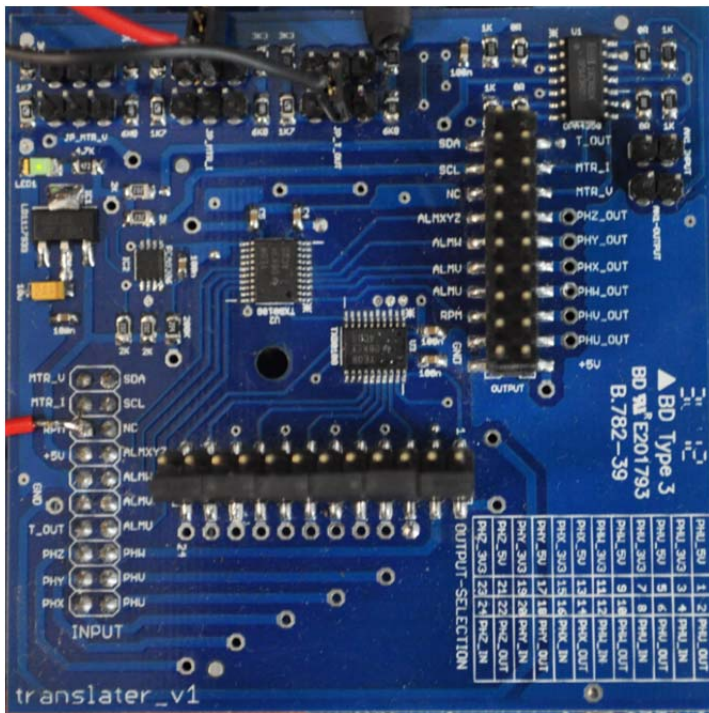


Figure 30: Translator Card

CHAPTER III

EVALUATION OF POWER ELECTRONICS MODULE

The power electronics part of the system consists of rectifier, inverter and isolation subsystems. After the successful system integration and implementation, the desired measurements for educational purposes can be performed. In this chapter, the most relevant signal outputs are shown and discussed for the power electronics part of the system.

3.1 EVALUATION OF RECTIFIER SUBSYSTEM

The rectifier subsystem consists of four modules, which are uncontrollable single phase rectifier, uncontrollable three phase rectifier, controllable single phase rectifier and controllable three phase rectifier. For testing the uncontrollable single phase rectifier, 220V AC RMS voltage is applied to the input and a 200R (resistive) load is connected to the output. The basic schematic is shown in Figure 31.

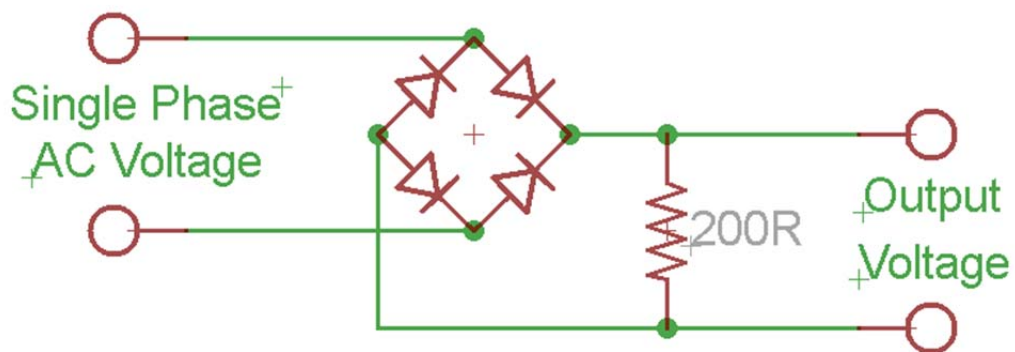


Figure 31: Single Phase Rectifier Test Circuit

The output voltage is shown in Figure 32. Since there is no capacitor connected to the output, the output is not a smooth DC voltage. When 220V AC RMS signal is rectified, peak value of DC voltage is 330V. If the required capacitor is connected to the output, a smooth DC voltage level of 217V is available at output. The capacitor included output signal is observed as shown in Figure 33.

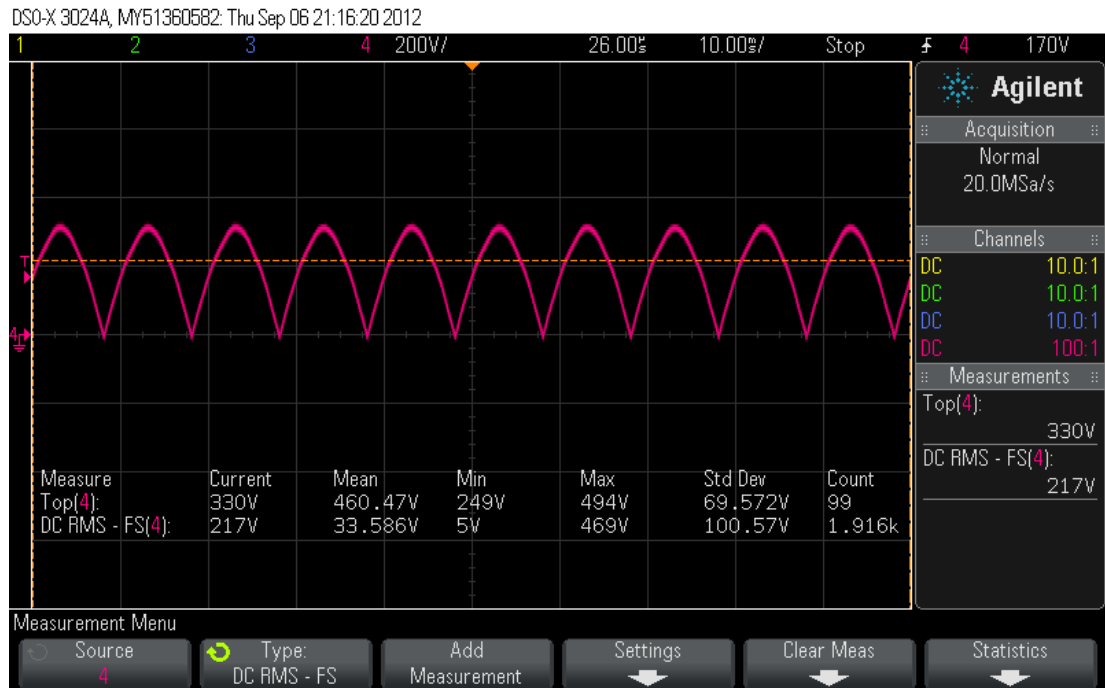


Figure 32: Single Phase Rectifier Output Voltage Without Capacitor

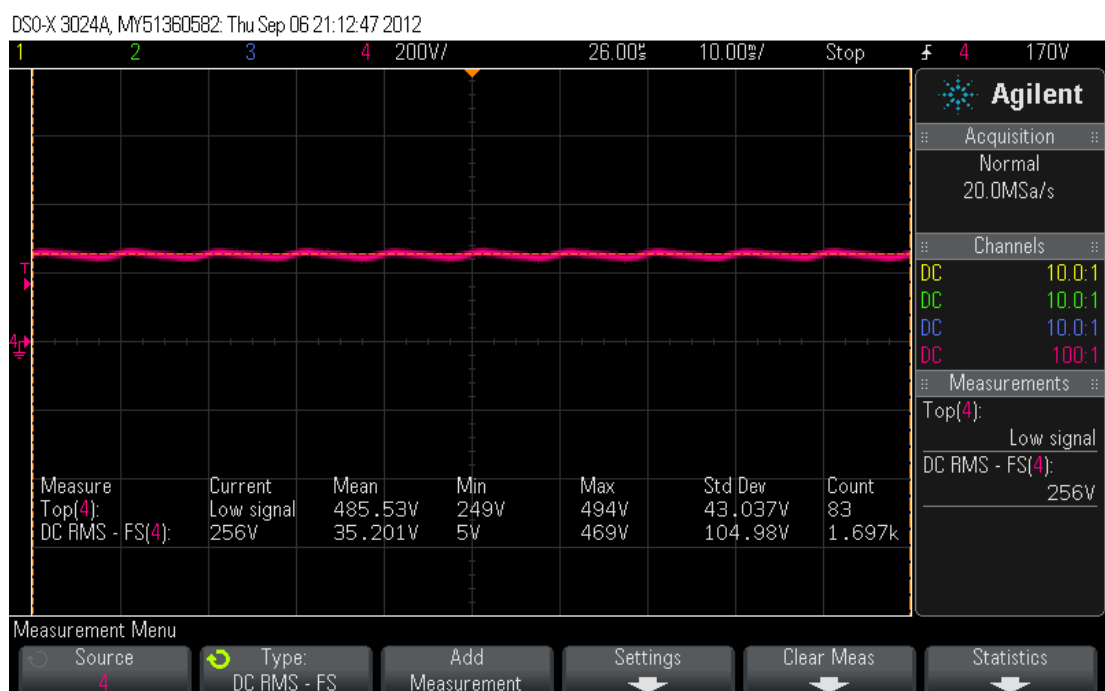


Figure 33: Single Phase Rectifier Output Voltage With Capacitor

For testing uncontrollable three phase rectifier, three phase 220V AC RMS voltages are applied to the inputs and 200R load is connected to the output. The basic schematic is shown in Figure 34.

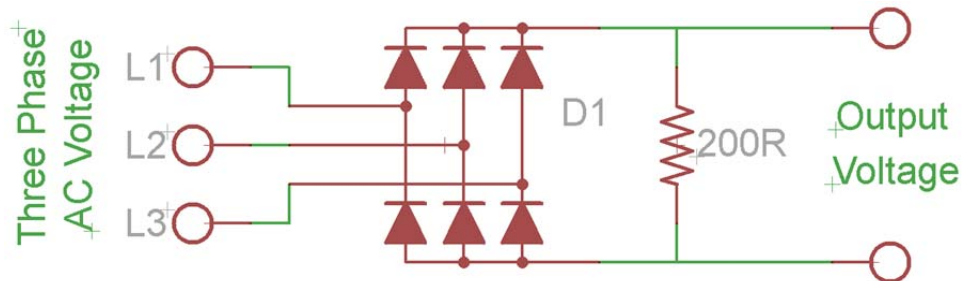


Figure 34: Three Phase Rectifier Test Circuit

The output voltage is shown in Figure 35. Since there is no capacitor connected to the output, the output is not a smooth DC voltage. When three phase 220V AC RMS signal is rectified, peak value of DC voltage is 494V.

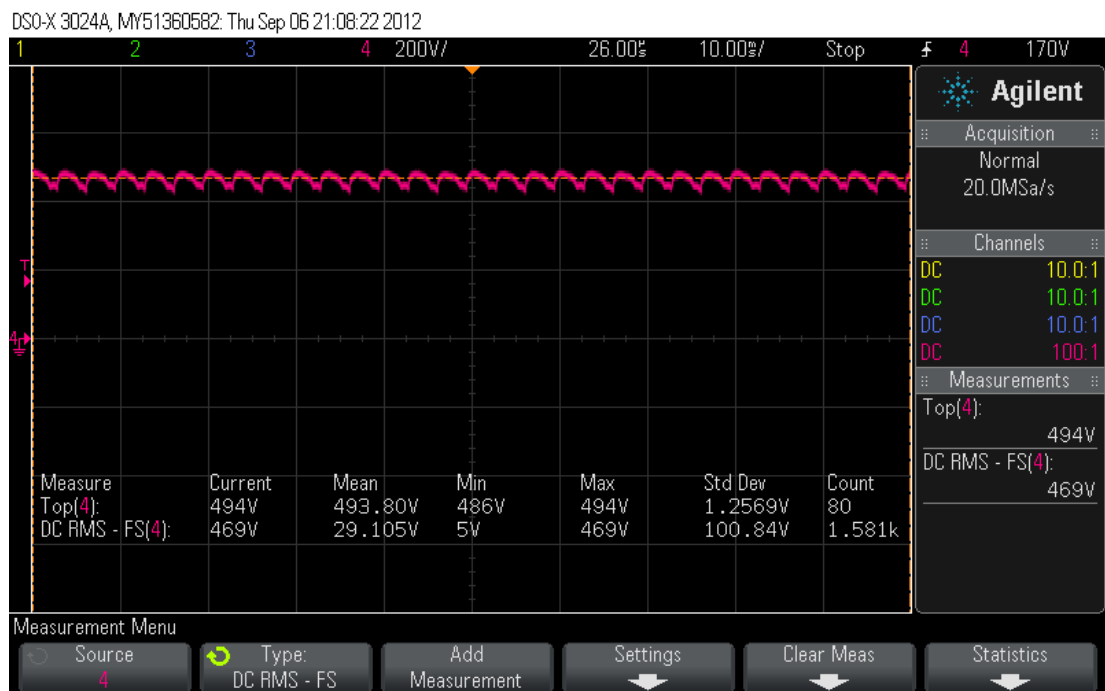


Figure 35: Three Phase Rectifier Output Voltage Without Capacitor

For testing controllable single phase rectifier, 220V AC RMS voltage is applied to the inputs and 200R load is connected to the output. The basic shematic is shown in Figure 36. The single phase thyristor controller module is used for triggering the gate inputs.

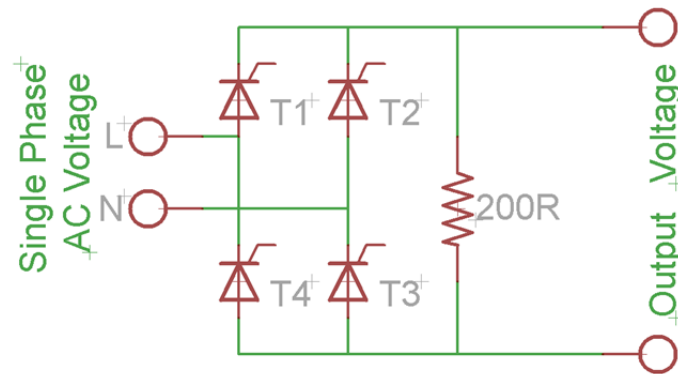


Figure 36: Controlled Single Phase Rectifier Test Circuit

The output voltage is shown in Figure 37. Since there is no capacitor connected to the output, the output is not a smooth DC voltage. When the controller analog voltage output is 0.58V, the maximum peak DC output voltage of 328V is observed on the oscilloscope. If the capacitor is connected to the output, a smooth DC voltage level of 217V is available at output. The output signal for the experiment with capacitor is observed as shown in Figure 38.



Figure 37: Controllable Single Phase Rectifier Output Voltage Without Capacitor

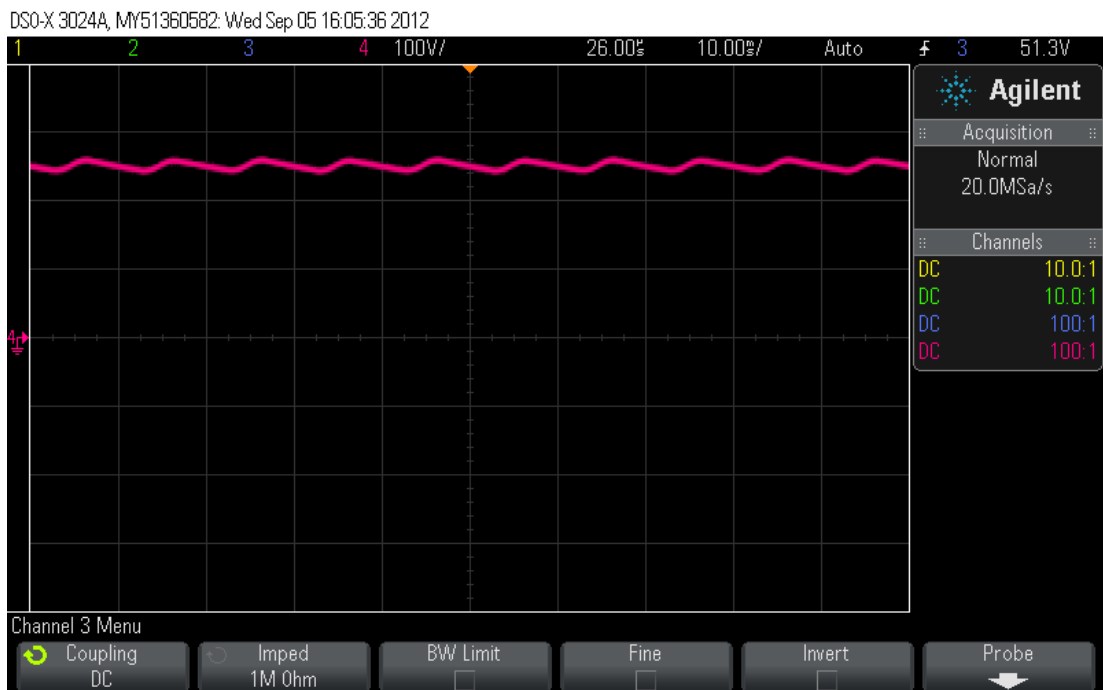


Figure 38: Controllable Single Phase Rectifier Output Voltage with Capacitor

For testing the controllable three phase rectifier, a three phase 220V AC RMS voltages is applied to the inputs and a 200R load is connected to the output. The basic shematic is shown in Figure 39. The three phase thyristor controller module is used for triggering the gate inputs.

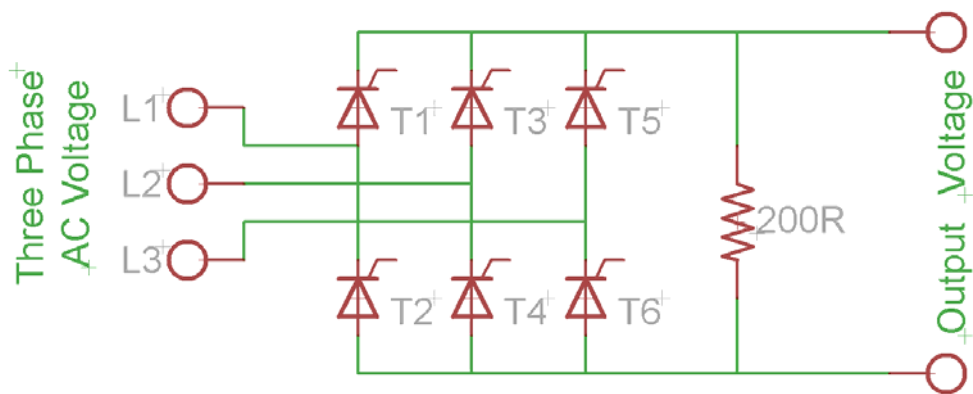


Figure 39: Controlled Three Phase Rectifier Test Circuit

The output voltage is shown in Figure 40. Since there is no capacitor connected to the output, the output is not a smooth DC voltage. When the analog voltage output of the controller module is 0.58V, a maximum peak DC output voltage of 494V is observed on the oscilloscope. If the capacitor is connected to the output, a smooth DC voltage level of 469V is available at output.

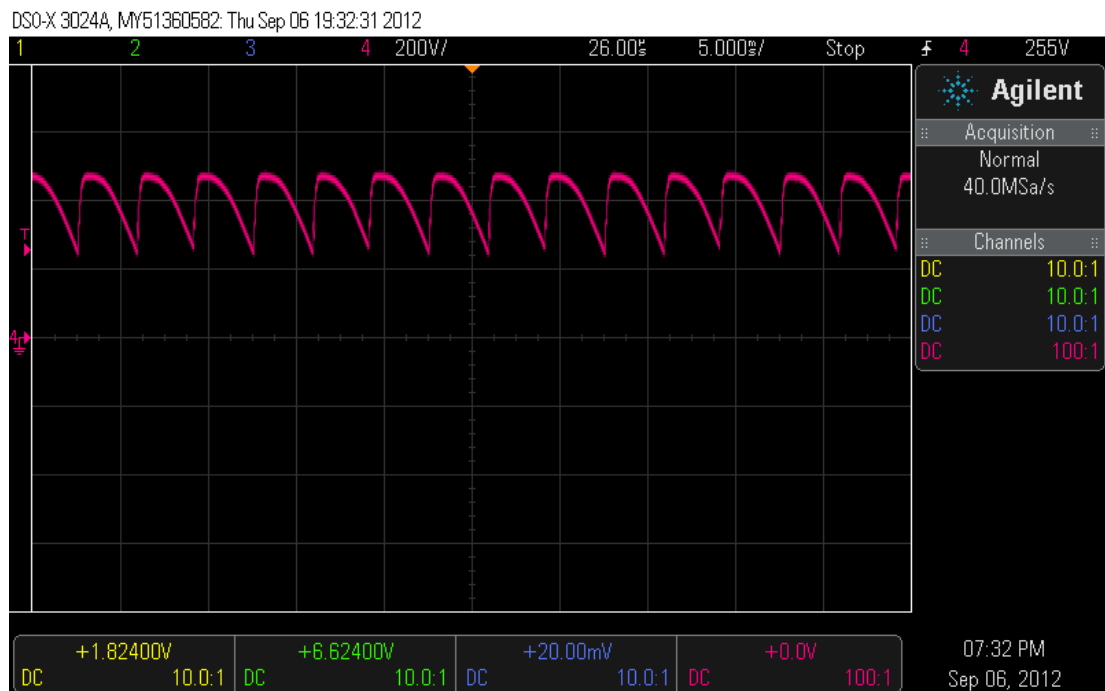


Figure 40: Controllable Three Phase Rectifier Output Voltage Without Capacitor

3.2 EVALUATION OF INVERTER SUBSYSTEM

The inverter part is an important subsystem where rectified DC supply voltage, control signals, output of the three phase signals and alarm signals are evaluated. Rectified DC supply voltage is discussed in the previous section and the control signals are discussed in chapter 4. In this section, output of the three phase voltage signals is observed for both delta and star connections of the AC motor. In case of a star connection, a three phase input voltage is applied to the stator inputs (U1,V1,W1), while the other three inputs (U2,V2, W2) are connected together to form the virtual neutral line. The star connection is illustrated in Figure 41. When the voltage is measured between line and the neutral, the phase voltage can be seen as shown in Figure 42. In this Figure, output of the system is noisy. Because capacitor is not connected to the output of the inverter. But noisy output is not important for the AC induction motor. This output is suitable for driving the AC motor.

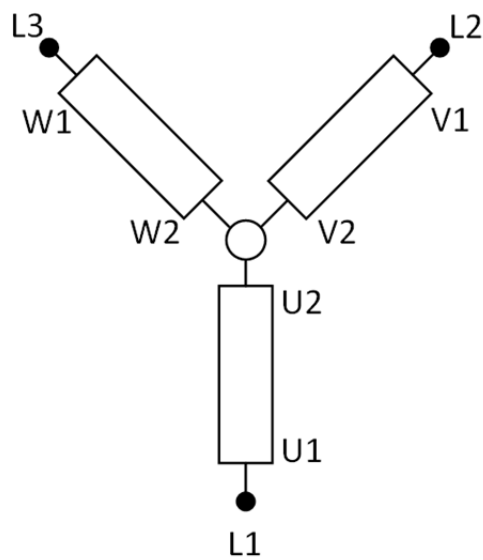


Figure 41: Star Connection for AC induction Motor

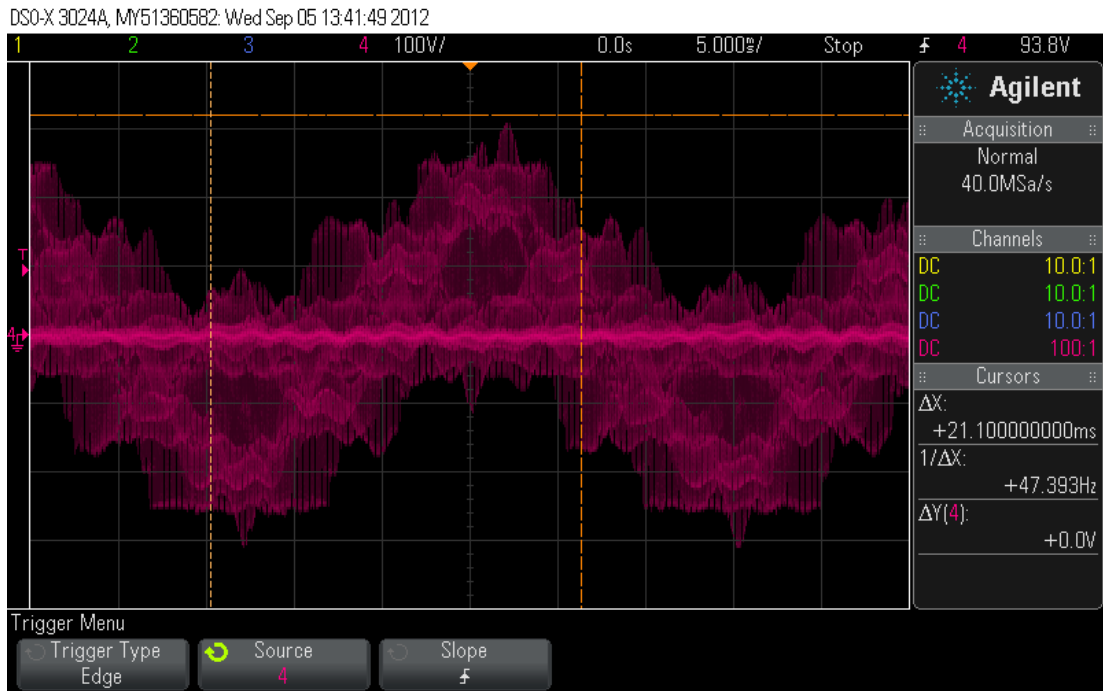


Figure 42: Inverter Output Voltage (Line to Neutral)

In the star connection, each stator voltage is 220V. In contrast, a delta connection is more powerful than the star connection, since each stator voltage is 380V. The delta connection is shown in Figure 43 and the line to line voltage measurement is depicted in Figure 44. In this figure, output of the inverter is observed. Hence, the end user learns that the output of the inverter is not sinusoidal without capacitor.

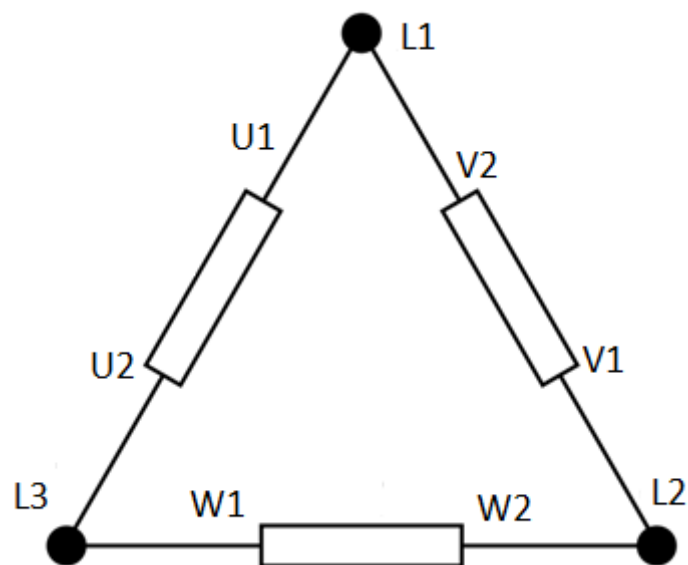


Figure 43: Delta Connection for AC Induction Motor

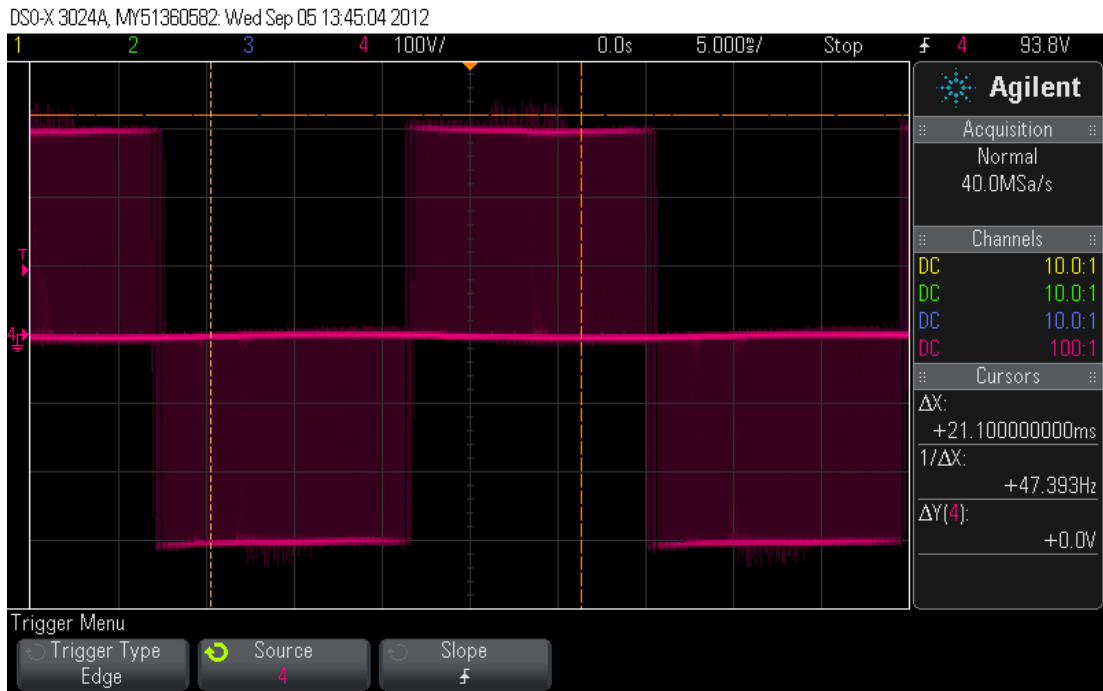


Figure 44: Inverter Voltage Output (Line-to-Line)

Star connection is used with mains AC voltage at the motor startup since a delta connection maintains high power due to the sink of high current. Usually a star connection is used at motor startup, since a delta connection may damage the motor. After startup, the connection is usually changed to delta. For this reason star connection is not used for variable frequency driver (VFD) which controls the speed.

CHAPTER IV

EVALUATION OF THE CONTROL MODULE

The controller subsystem is the most valuable part of the system. All control system algorithm are running on the microcontroller. Scalar control method and SPVM as described in Chapter 2 are used for open-loop speed control of the motor. However, if closed-loop speed control is desired, a plant model should be identified. For this reason, the AC motor model, system plant model, step response of the open loop system, step response of the closed loop system and different controller designs are discussed in this chapter. In addition, various experiments are performed and the measurement results are discussed.

In this research V/F control is used for controlling the AC induction motor. Also SVGEN is used for generating the PWM signals for the inverter which are shown in Figure 45. These signals are the upper IGBT's gate inputs (cf Figure 14). The inverted upper IGBT's gate input signals are applied to the lower IGBT's gate inputs. These PWM signals control the inverter for generating the three phase AC voltage.

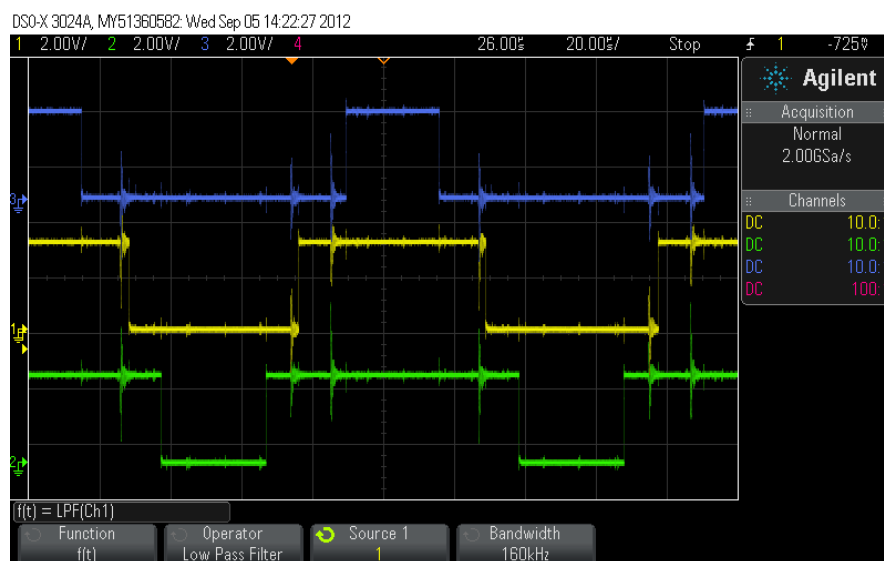


Figure 45: PWM Signals (Upper Side IGBT) for Controlling the Inverter

4.1 PLANT MODEL IDENTIFICATION

In this research, the system plant consist of the AC induction motor and the open-loop control implementation of the F28035 DSP controller as it was shown in Figure 27. F28035 DSP is used for safe acceleration of the AC induction motor in order to avoid large peaks of the motor current. In order to perform feedback controller design, a model of the plant should be obtained. In this thesis, the MATLAB identification toolbox is used for identifying the system plant from a step response measurement. The result of the identification is the plant transfer function. The plant transfer function used for identification is shown in equation 4.1.

The identification toolbox needs measured inputs and output values for determining the transfer function coefficients. The system input is phase frequency (Hz) and the system output is speed (RPM). The desired phase frequency and the motor speed values are measured at the same time and the synchronous data are used for identifying the plant model.^[29]

$$\text{Tr}(s) = \frac{K_t}{as^2+bs+c} \quad (4.1)$$

For this research, D-LAB is used for logging the phase frequency and motor speed at the same time. At the beginning of the experiment, the desired phase voltage is 35Hz, and it is instantly increased to 50Hz in the form of a step input. Simultaneously, the motor speed is 1050rpm, at the beginning, and its dynamic response increases to 1500rpm. The phase voltage (plant input) is shown in Figure 46 and the motor speed (plant output) is shown in Figure 47.

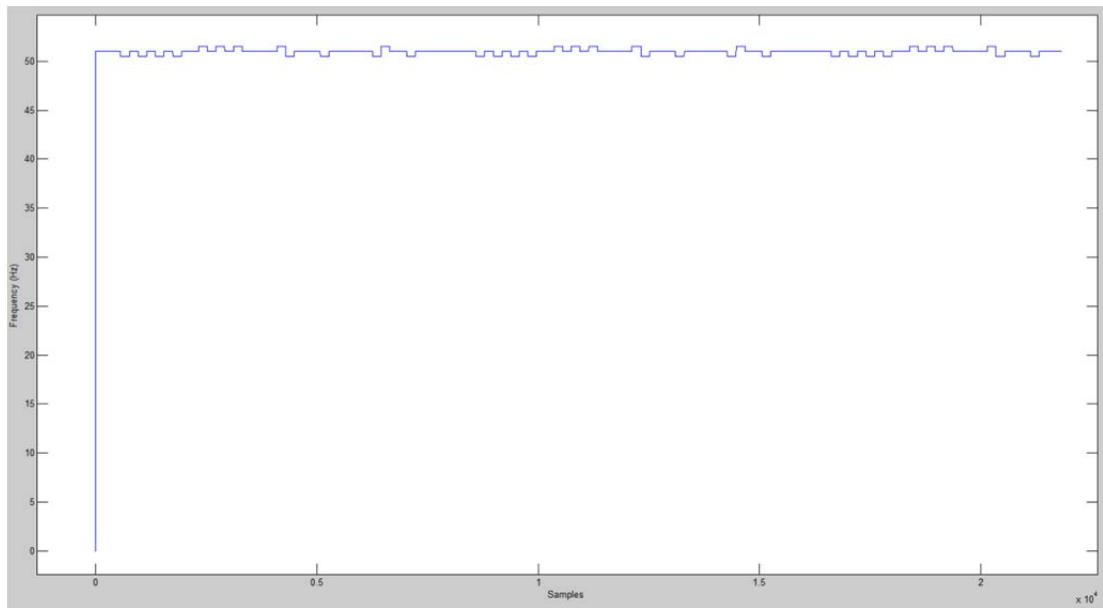


Figure 46: Desired Phase Frequency Graph (Plant Input) for Acceleration

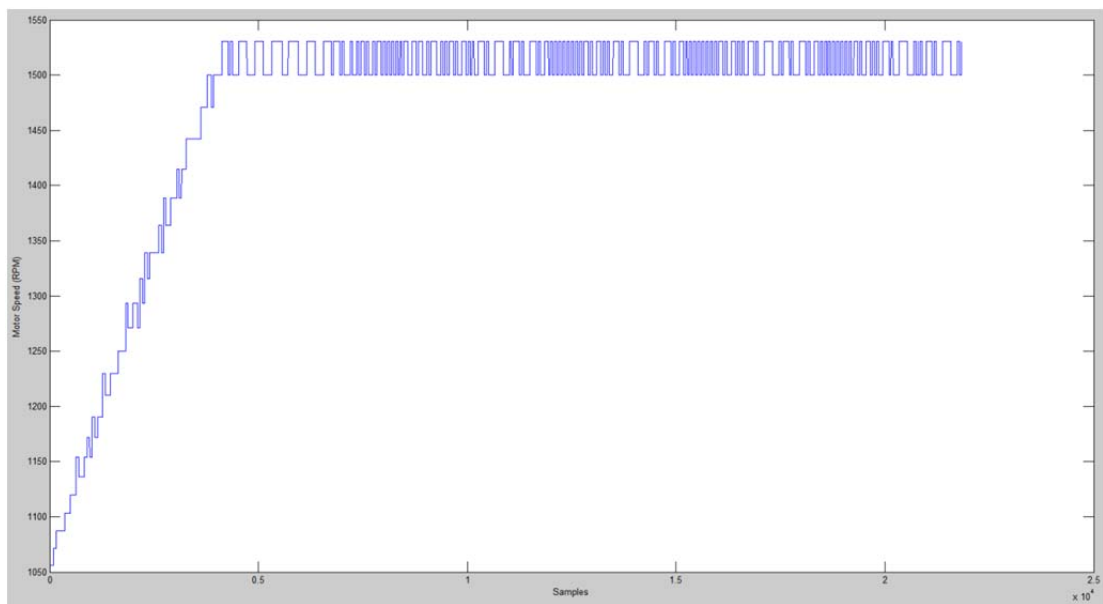


Figure 47: Motor Speed Graph (Plant Output) for Acceleration

These values are used in the MATLAB identification tool for identifying the system plant model. This tool matches the measured step response with the step response of the identified transfer function. Afterwards, the system plant transfer function coefficients can be exported. The output of the MATLAB identification tool is shown in Figure 48. Also the graph of the open loop system step response is shown in Figure 49.

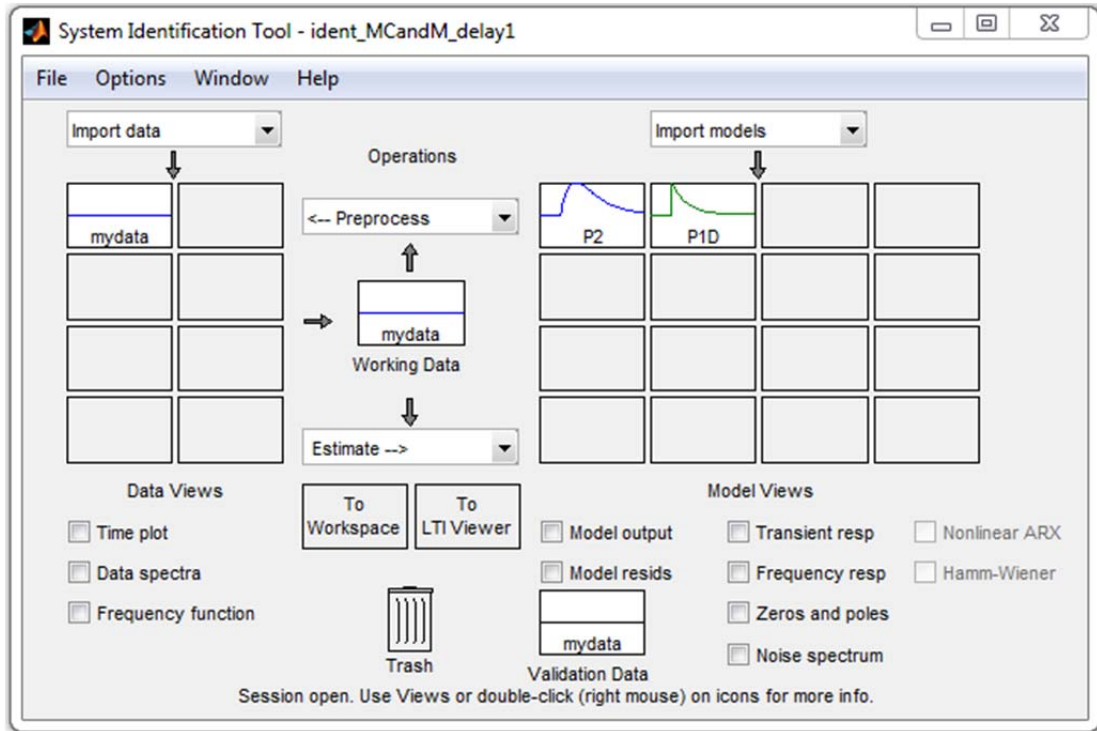


Figure 48: Output of The MATLAB Identification Fitting Tool

The following transfer function coefficients are found by the identification tool. They are $a=1$, $b=10.03$, $c=25.16$ and $K=749.1$. Then, Equation 4.1 is used for finding the transfer function of the plant.

After the identification, the system plant model is validated. To this end, the output of the system (motor speed) and the step response of the plant transfer function are drawn in the same figure. If the step response follows the output of the system, the system plant model is validated. This validation is shown in Figure 50. The blue line is the step response of the plant. The red line is the output of the system.

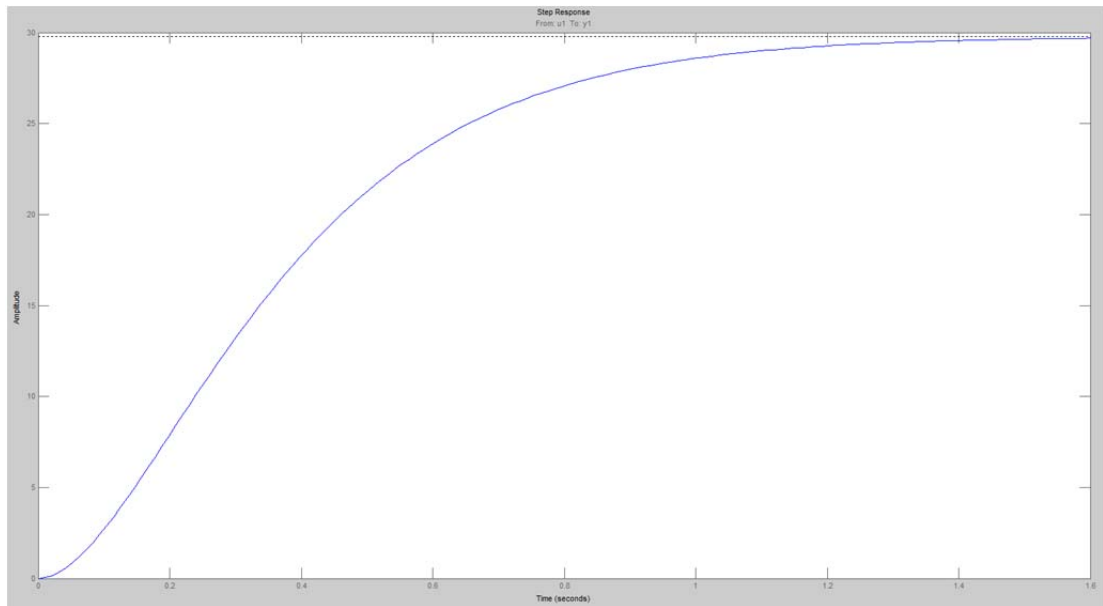


Figure 49: Open Loop System Step Response

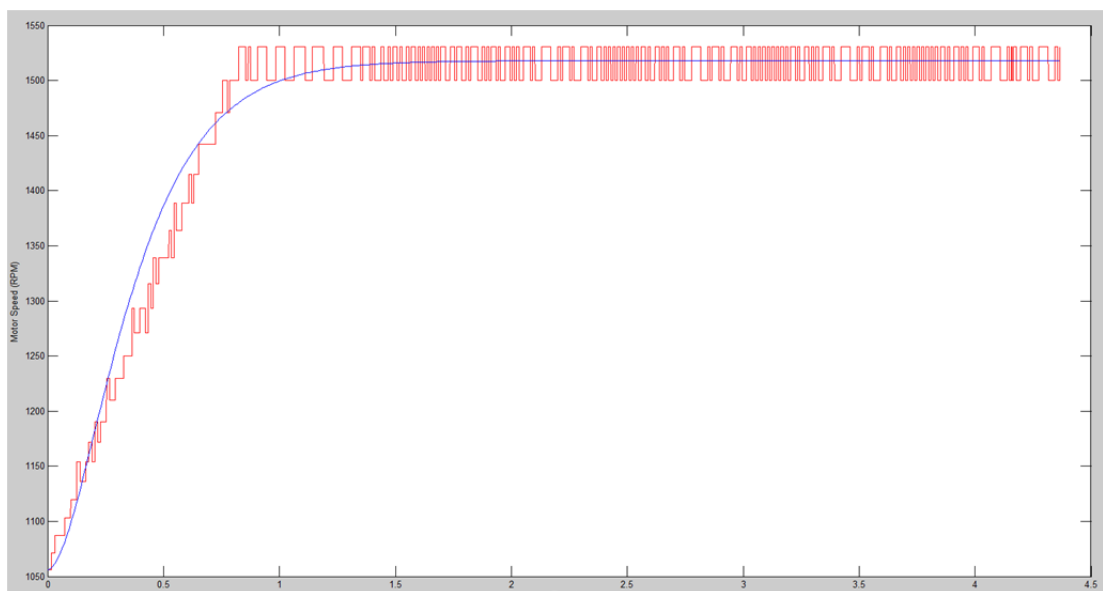


Figure 50: Plant Model Validation

The AC induction motor phase frequency and the output of the motor speed is used for finding AC induction motor model. The motor phase frequency is the input and the motor speed is the output. The input and output values are used in the MATLAB identification tool for finding the AC induction motor step response, which is shown in Figure 51. Also this tool gives the coefficient of the AC motor transfer function. In this case, $a=1$, $b=1040$, $c=3.978e4$ and $K=1.184e6$. In order to get this result, equation 4.1 is used for finding the transfer function of the AC motor.

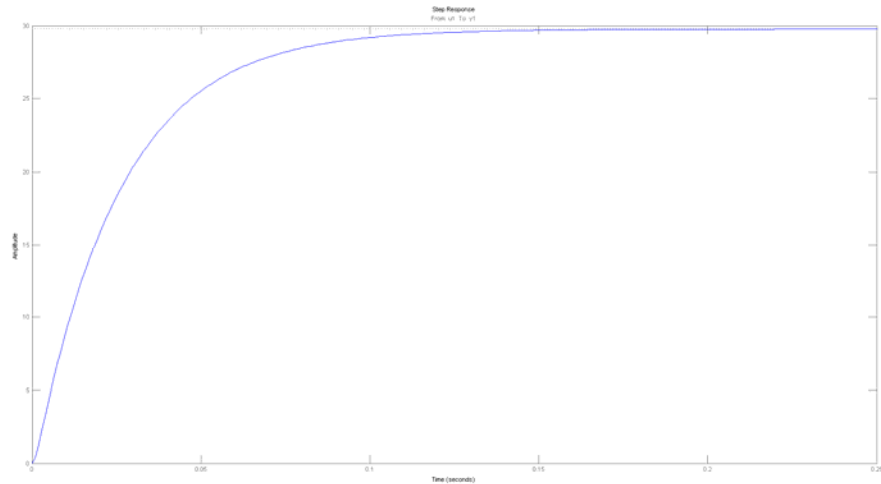


Figure 51: AC Induction Motor Step Response

The AC induction motor model and the system plant model are compared in the same figure, and the differences between the models are shown. The system plant is slower than the motor because the DSP is programmed to increase the motor speed slowly. The reason for this is that the motor sinks current when it runs. That is, if it accelerates instantly, it may damage itself. The differences of the models is illustrated in Figure 52.

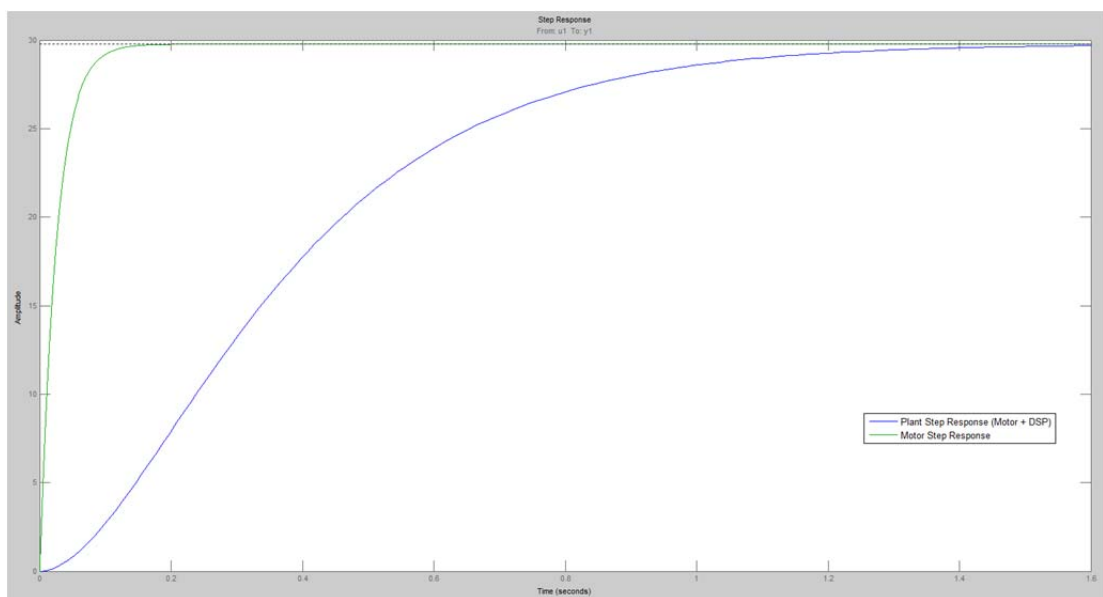


Figure 52: Differences of The AC Induction Motor and Plant Model

4.2 CONTROLLER DESIGN

PID (Proportional + Integral + Derivative) control is the most widely used control strategy in process industries. PID controller attempts to reduce the error by adjusting the process control inputs. For this reason, PID controller is chosen to control this research system. A basic feedback control is shown in Figure 53. PID controller consists of proportional, integrational and derivative parts which are shown in Figure 54. The proportional part multiplies a constant value to the error signal. This constant value's name is K_p . As a result of the multiplication, the response time increases. But If the proportional gain is too much, the system may become unstable. The integration part integrates the error signal in order to increase the response time. But it's effect is smaller than the proportional part. Also it decreases the ess (error steady-state). K_i is the name of the integrative gain constant. The derivative part derivates the error signal for decreasing the settling time. If there is too much ripple in the error signal, the derivative part is applied. K_d is the name of derivative gain constant. These constants are declared in equation 4.2. The PID parameters, which are K_p , K_i and K_d , must be found for each process (system). In this thesis, pole placement method is used for finding the PID parameters.^[29]

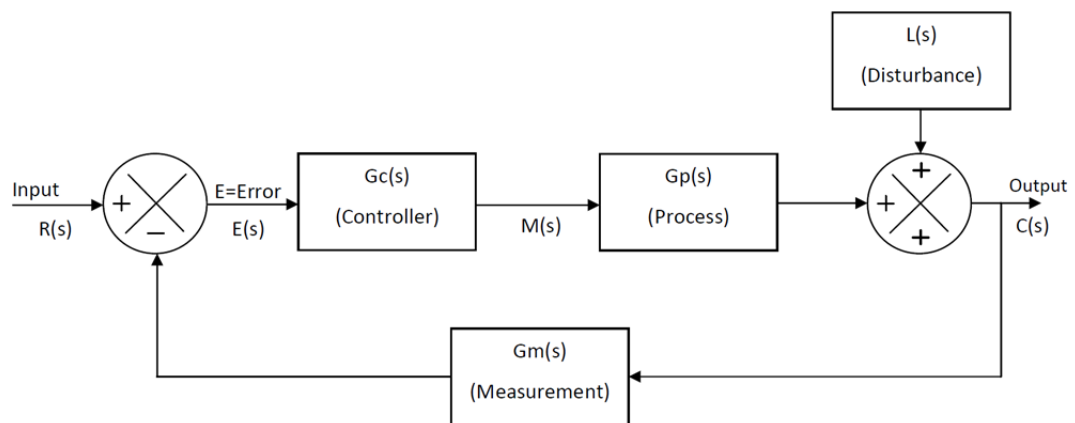


Figure 53: A Basic Feedback Control System

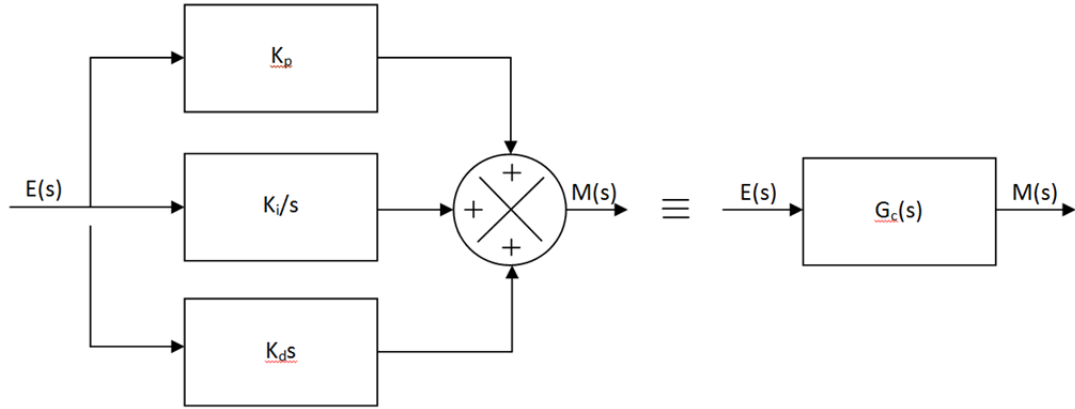


Figure 54: The Ideal PID Controller

$$G(s) = K_p + \frac{K_i}{s} + K_d s \quad (4.2)$$

4.2.1. Pole Placement Method

Pole placement method is used for finding PID parameters. In this research, the pole placement method is applied in the Laplace domain. Firstly, the desired PO (percent overshoot) and t_s (settling time) is decided. Formulation for these parameters are shown in equation 4.4 and 4.5. They are also shown in figure 55. Then “ ζ ” and “ ω_n ” are found by PO and t_s . “ ζ ” is the damping ratio of the system and “ ω_n ” is the undamped natural frequency. After that, the closed loop transfer function (CLTF) of the desired second order unity feedback system, has its formula shown in equation 4.3, the poles are found by using “ ζ ” and “ ω_n ”. For this research, the desired system requirement is selected as PO is 15% and t_s is 1 second.^[29]

$$G(s) = \frac{\omega_n}{s^2 + 2\xi\omega_n s + \omega_n^2} \quad (4.3)$$

$$PO = 100e^{\frac{-\xi\pi}{\sqrt{1-\xi^2}}} \quad (4.4)$$

$$t_s \approx \frac{4}{\xi\omega_n} \quad (4.5)$$

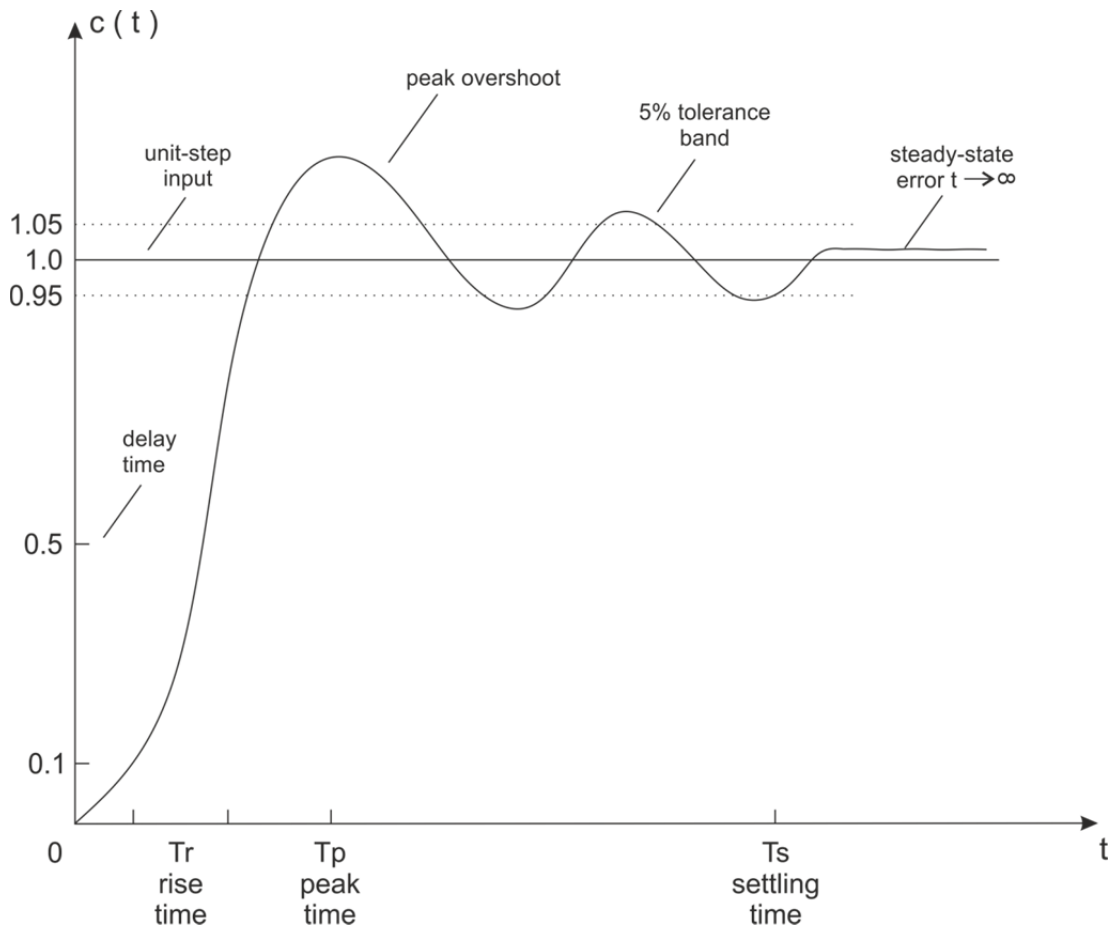


Figure 55: Unit Step Response

When ξ and ω_n are found, the desired second order system equation is generated. This equation represents the characteristic polynomial of the closed-loop system. Using this polynomial, the PID parameters are found by solving two equations together. The system plant model is found in chapter 4. System open loop transfer function consists of the PID compensator and the plant transfer function. The closed loop transfer function is calculated by equation 4.6.^[29]

$$CLTF = \frac{G}{1+G} \begin{cases} G = G_p \times G_c \\ G_p: AC \text{ motor transfer function} \\ G_c: PID \text{ compensator} \end{cases} \quad (4.6)$$

The calculated CLTF of the system is shown in equation 4.7. 'a', 'b', 'c' parameters are coefficient of the system plant transfer function. After the calculation, the desired

second order transfer function equate the calculated CLTF of the system. As a result of the equations, the PID parameters are found. which are $K_p=0.18$, $K_i=1$, $K_d=0.014$.

$$CLTF(s) = \frac{(K_t + K_d)s^2 + (K_t K_p)s + K_t K_i}{as^3 + (K_t K_d + b)s^2 + (K_t K_p + c)s + K_t K_i} \quad (4.7)$$

The step response of the designed closed loop system is shown in Figure 56. As it is seen in the figure, "PO" and "ts" are under the desired values which indicated that the compensator design has succeeded.^[29]

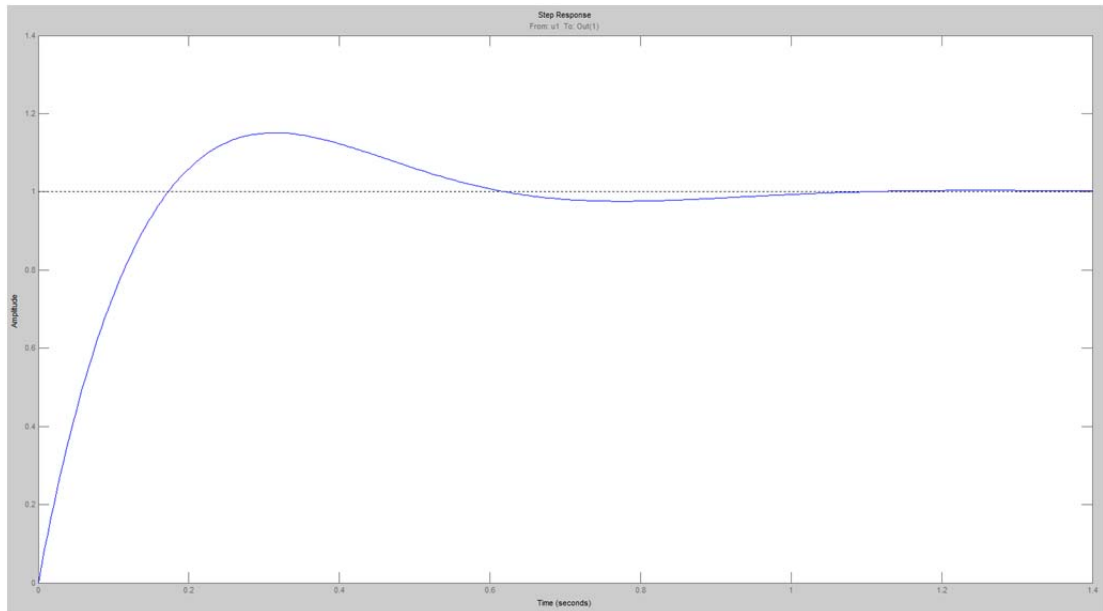


Figure 56: The Step Response of Closed Loop System

After the simulation, these PID parameters are applied to the real AC motor system without load. Accordingly, the output of the system is expected to resemble the simulation. However, the output of the system is slightly different than the simulation. This is because of model uncertainties that usually appear in practical systems but that do not exist in the simulation. In this case, the theoretical calculation results are not as same as the practical values. In any case, the practical closed-loop result is similar to the theoretical outputs. If the output of the system is

observed in Figure 57, the success of the closed loop PID control is shown. As it is seen in Figure 58 which shows all simulation results and real time data together, the controller design and validation are successful.

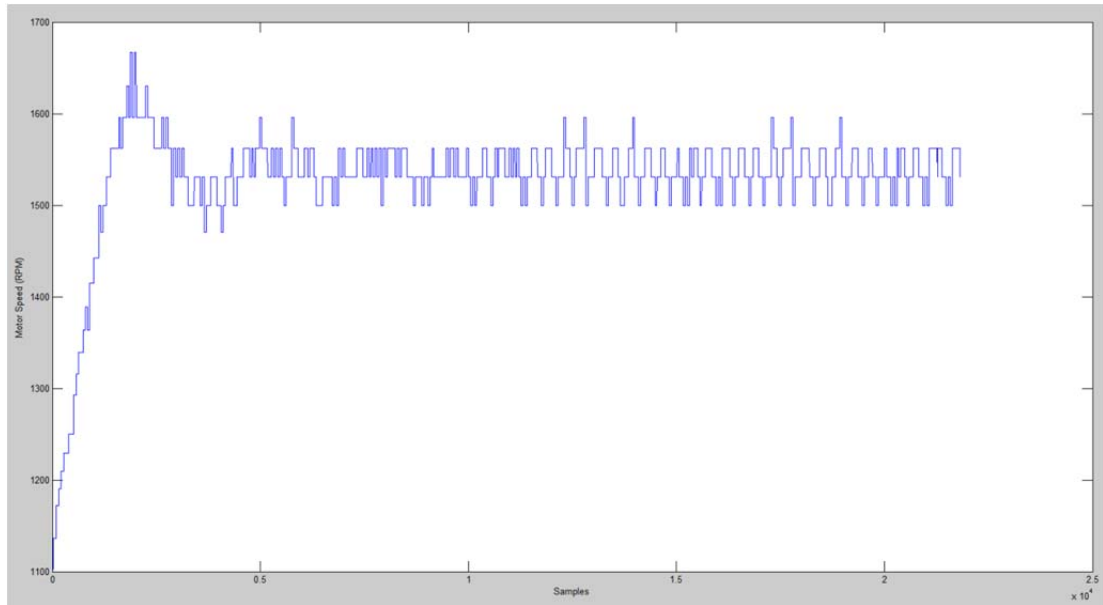


Figure 57: Closed Loop System Output with PID Control

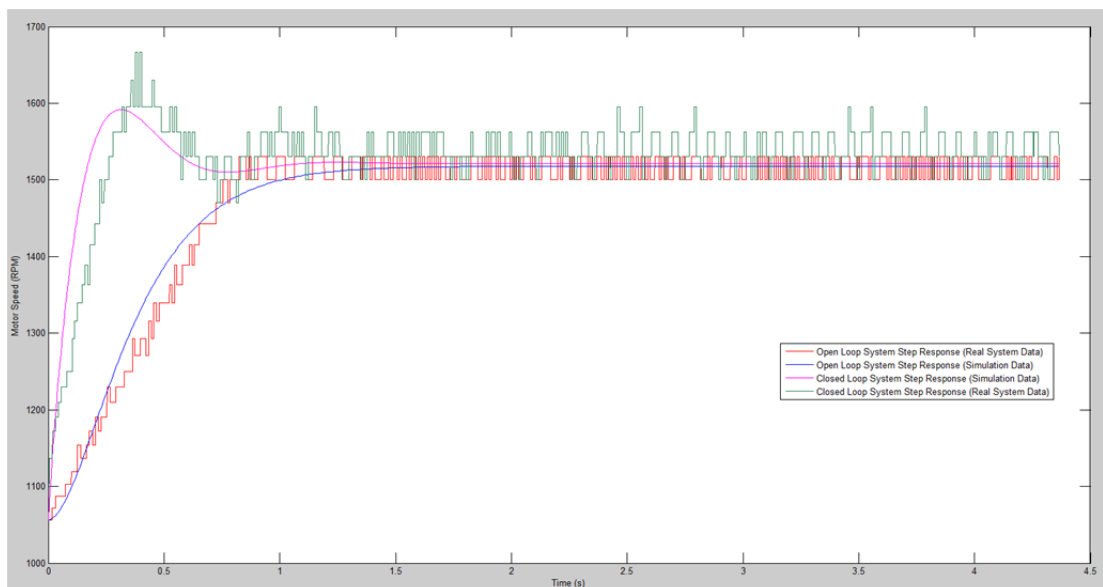


Figure 58: Simulation and Real Time System Validation

4.3 EVALUATION RESULTS OF THE SYSTEM

In the previous section, there was no load in the system, therefore there was no disturbance. In this section, a magnetic powder brake is used in order to apply a disturbance in the form of a load torque. Hence, it is possible to observe the behaviour of the controlled AC induction motor under load. Also the parameters of the AC induction motor with both speed and torque controllers are discussed in this section.

4.3.1. Behaviour of AC Induction Motor

For observing the behaviour of the AC induction motor, an open-loop system is used. This system is shown in Figure 59. In this case, system consists of a AC induction motor and a magnetic powder brake. For observation, a constant phase frequency is applied to the AC induction motor. Then the AC induction motor is loaded by the MPB. When the system is loaded by a small load, the AC motor speed decreases a little bit but still works. In this case, the AC motor phase frequency does not change because the system is an open-loop system. Also the DC input voltage decreases a little bit because of the load. These situations are shown in Figure 60. If the load is too high, the AC motor stalls. That is, the AC motor speed slows down to zero RPM. Also the DC input voltage decreases because of the load. This situation is shown in Figure 61.

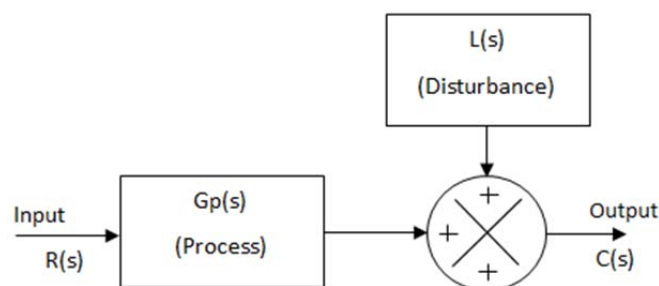


Figure 59: Open-Loop System with Disturbance

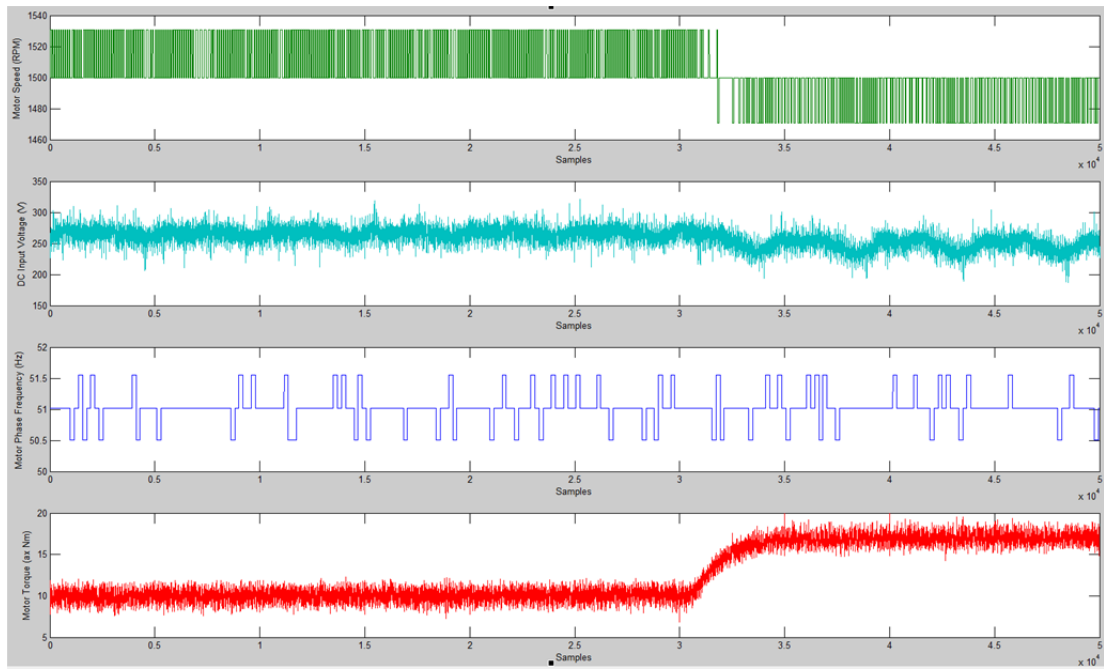


Figure 60: Behaviour of the AC Motor under a Few Load

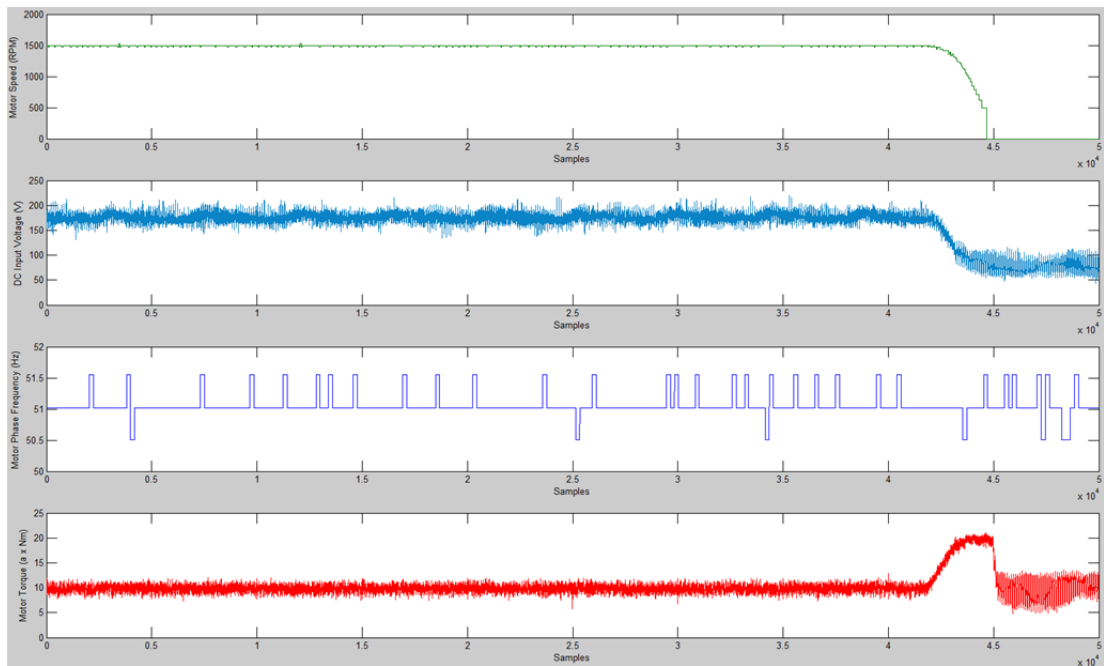


Figure 61: Behaviour of the AC Motor under High Load

4.3.2. Behaviour of The AC Induction Motor with Feedback Control

For observing the behaviour of the AC induction motor with the PID feedback controllerThe system is shown in Figure 62. In this case, the system consists of the AC induction motor with the speed controller and a magnetic powder brake. For observation, a reference phase frequency is applied to the AC induction motor. Then AC induction motor is loaded by the MPB. When the system is loaded by a small load, the AC motor speed does not change because of the speed controller. In this case, the AC motor phase frequency is automatically adjusted by DSP. Also, theDC input voltage decreases a little bit because of the load. These situations are shown in Figure 63. Even if the load is approximately equal to maximum motor torque (critical load), the AC motor continues to run at the specified speed.This situation is shown in Figure 64. That is, the load that stalls the motor in the open-loop case can be tolerated in the feedback control case.

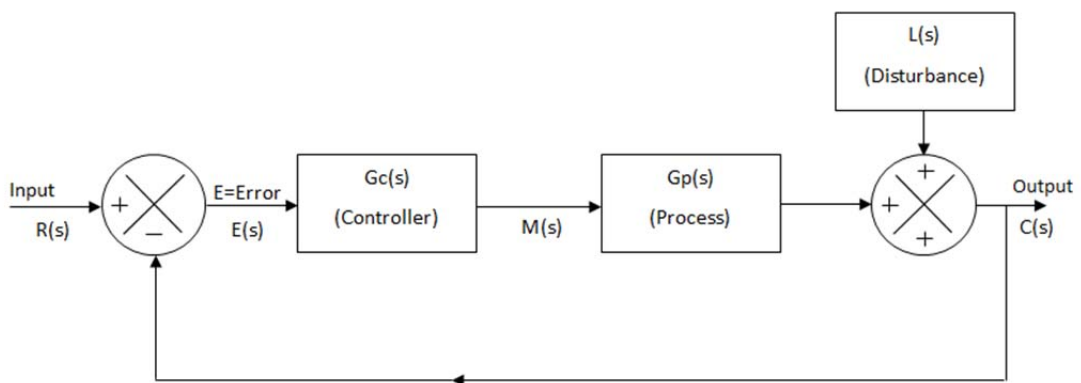


Figure 62: Closed-Loop System with Disturbance

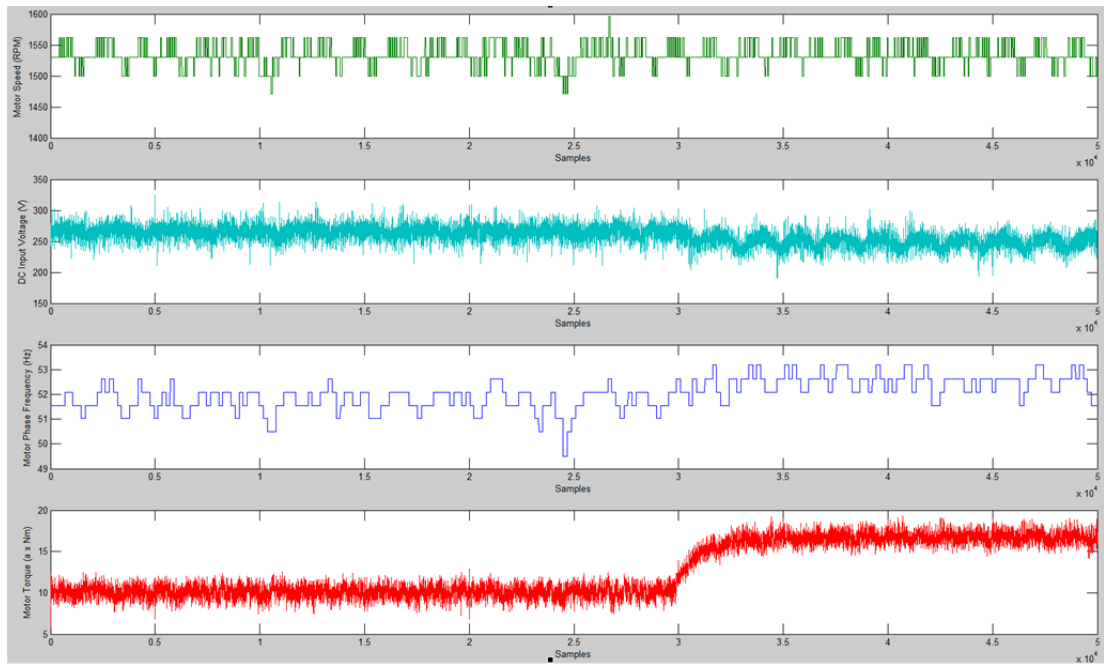


Figure 63: Behaviour of the AC Motor with the Speed Controller under a Small Load

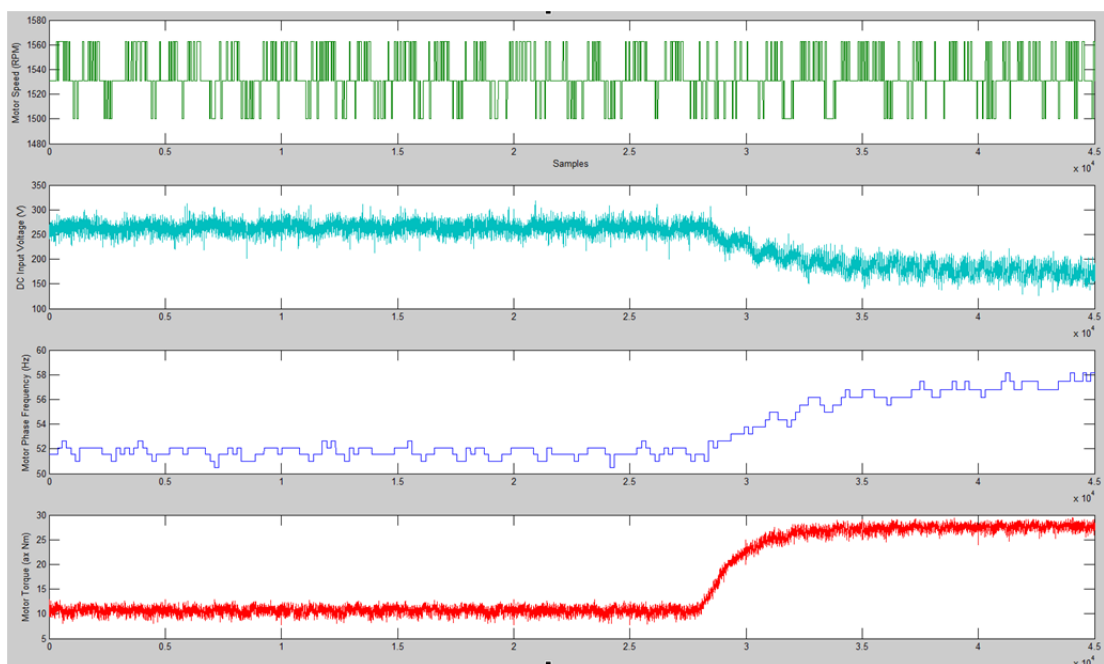


Figure 64: Behaviour of the AC Motor with the Speed Controller under Critical Load

4.3.3. Behaviour of The AC Induction Motor with Speed and Torque Control

The DC input voltage limits the maximum torque in the system. That is, the maximum torque can be controlled by adjusting the DC voltage. In particular, if the DC voltage input value is maximum, the motor torque limit is maximum. But if the system does not need the maximum torque limit, it is waste of power. Because of this reason, it is proposed to establish power efficiency by controlling the DC input voltage level of the inverter. By this way, the maximum torque limit is controlled. The DC voltage input is adjusted by the rectifier which is controlled by applying an analog voltage level between 0 to 5VDC. This analog voltage is generated by F28035 DSP. In this system, look up table is used for controlling the maximum torque limit.

The look up table values, which are measured from the system, are shown in table 2. Normally rectifier module are controlled by reference module. Reference module control signal output is 0 to 10VDC. Also reference module is controlled by manual or analog voltage level. This analog voltage level is 0 to 5VDC and also it is generated by DSP. Hence, rectifier reference voltage is shown in table 2.^[29]

In the feedback loop with torque control, the torque value is measured by the torquemeter as an input for the F28035 DSP. Then the DSP adjusts the DC voltage input value according to the required maximum torque in the look up table. The control system always adjusts the DC voltage value with a slightly larger voltage value in order to establish a higher torque value than the critical torque. The main result of this procedure is to keep the motor running as the motor torque changes instantly.

For observing the behaviour of the AC induction motor with the torque controller, a closed-loop system is implemented. This system is shown in Figure 62. In this case, the system consists of the AC induction motor with the torque controller and a magnetic powder brake. For observation, a constant phase frequency is applied to the AC induction motor, whereas the DC Input voltage is adjusted by the DSP. Then the AC induction motor is abruptly loaded by the MPB. When the system is loaded by a small load, the AC motor speed decreases a little bit but still works. In this case, the DC input voltage is increased by the DSP when the AC motor is loaded. These situations are shown in Figure 65.

Reference Voltage of Rectifier	Torque (a x Nm)	DC Supply Voltage
5.087	28	285
5.204	24	281
6.034	22	275
6.147	21	268
6.312	20	262
6.4	19	259
6.45	18.6	256
6.5	18.3	253
6.55	18	250
6.6	18	250
6.7	17.7	241
6.8	17.4	236
6.9	16	231
7	14	225
7.1	13	221
7.2	12	210
7.3	12	206
7.4	11	194
7.5	10	188
7.6	10	177
7.7	9	166
7.8	8	154
7.9	7	143
8	6	137
8.1	5	128
8.2	4	116
8.3	3	0

Table 2: Look Up Table for Maximum Torque Limit

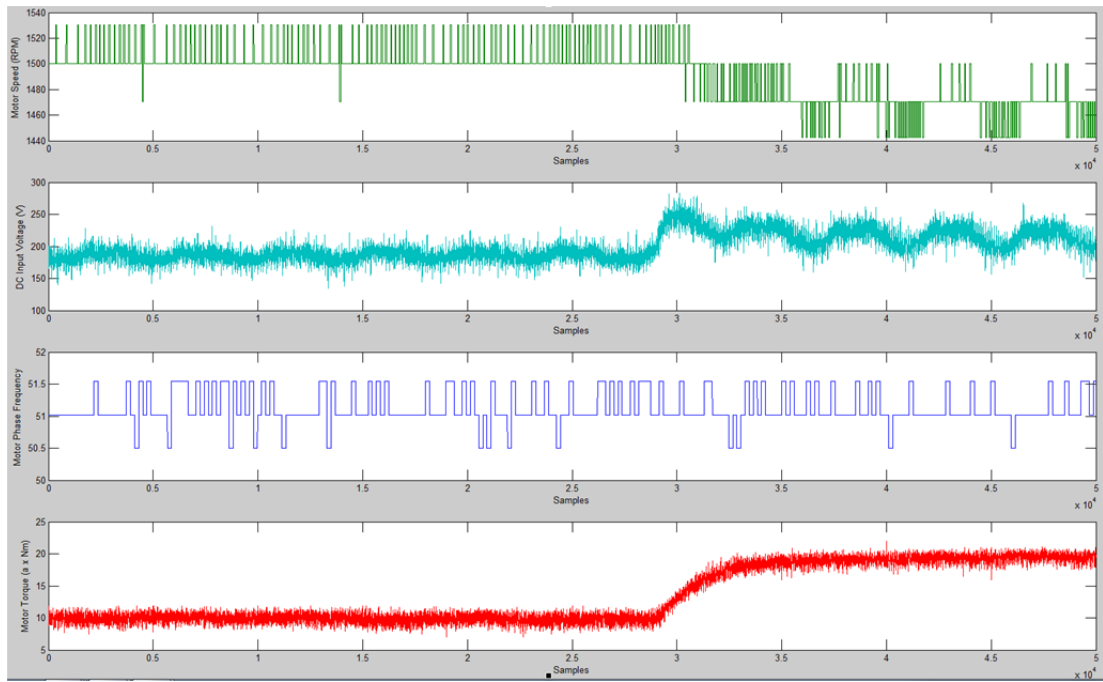


Figure 65: Behaviour of the AC Motor with the Torque Controller under a Small Load

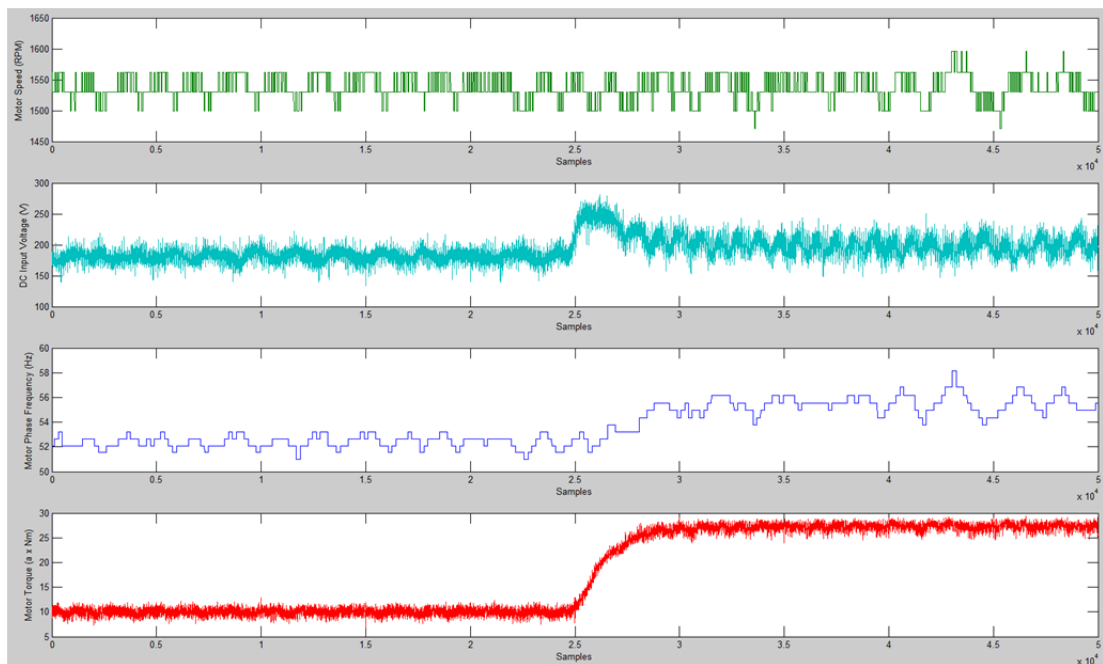


Figure 66: Behaviour of the AC Motor with the Speed and Torque Controllers under the Critical Load

Finally, torque control and speed control are combined in order to achieve constant speed without break down. For observing the behaviour of the AC induction motor with the speed and torque controllers, a closed-loop system is used. This system is shown in Figure 62. In this case, the system consists of the AC induction motor with the speed and torque controllers and a magnetic powder brake. For observation, a reference phase frequency is applied to the AC induction motor. Also the DC Input voltage is adjusted by the DSP. Then the AC induction motor is loaded by the MPB. Even if the system is loaded by the critical load, the AC motor speed does not change because of the speed controller. In this case, the DC input voltage is increased by the DSP when the AC motor is loaded. These situations are shown in Figure 66. It has to be remarked that this control loop uses two independent controllers. SISO speed control is performed using the speed measurement. In addition, the torque limit is adjusted based on the torque measurement.

If the load is higher than the maximum motor torque limit, the AC induction motor stalls. In that case, the AC motor speed slows down to zero RPM. At the same time, the motor phase frequency is increased by DSP and the DC input voltage is increased up to the maximum level. However, the speed and torque controllers do not help for keeping the speed at the same level. Also the DC input voltage decreases because of the load. These situations are shown in Figure 67.

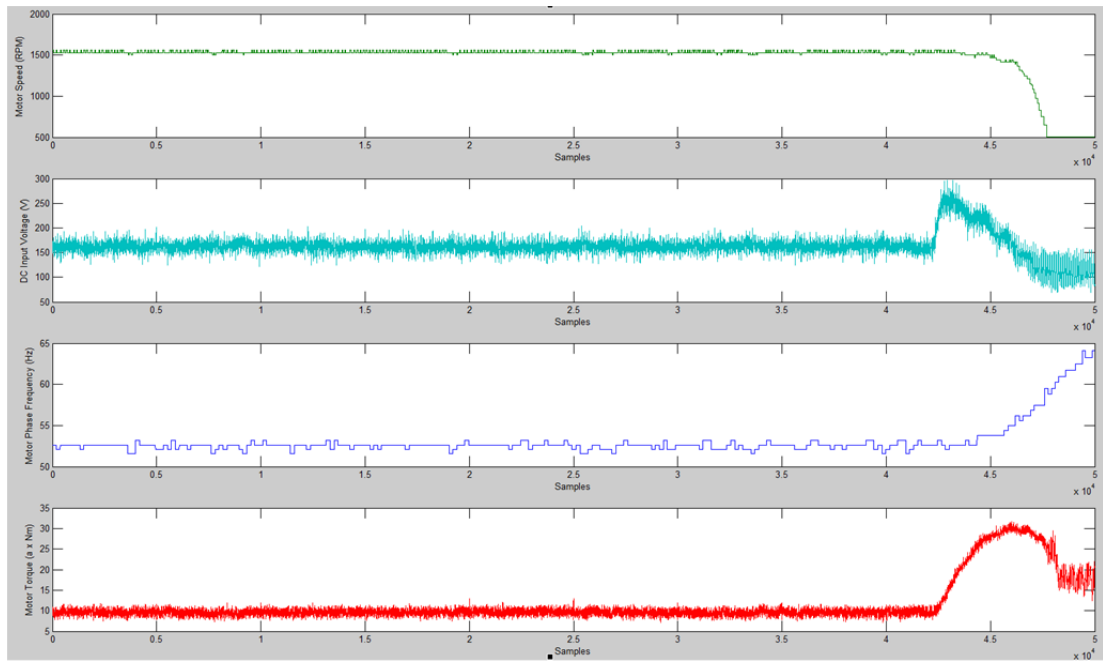


Figure 67: Behaviour of the AC Motor with the Speed and Torque Controllers under High Load

CONCLUSION

In this research, all goals are achieved. An AC induction motor driver training set is designed for students and educators. This training set allows to both conduct power electronics experiments as well as feedback control experiments. Accordingly, the training set consists of a controller subsystem and a power electronics subsystems which are designed modularly. All desired measurements are observed in the both subsystems.

In the power electronic subsystem, 4 types of rectifiers are designed for supplying the desired DC voltage. They include both uncontrolled and controlled rectifiers. In addition, an inverter is designed for driving the AC induction motor. This inverter is based on IGBT transistors and is suitable for up to 4KW AC induction motors.

In the controller subsystem, the F28035 DSP is used. The V/F (voltage/frequency) control method is applied to the motor and the space vector modulation principle is used in order to generate suitable PWM signals. Control experiments are conducted based on a system plant and motor model that is obtained based on real time measurements. In this context, MATLAB is used for model identification and control system simulation. A PID controller for reference steps and disturbances is designed with pole placement method. Very good agreement between the simulation experiments and the hardware measurements is obtained. In addition, the maximum torque limit of the motor is controlled by adjusting the DC voltage of the rectifier.

In the scope of this thesis, the AC induction motor driver training set design is completed. Students and educators have a new training platform for investigating power electronic components and to perform control with an AC motor case study. Users can apply different control methods or may change controller parameters for experimentation. Throughout this thesis, the design steps and algorithms are given with the methodologies used in this research.

REFERENCES

- [1] 12-Bit Digital to Analog Converter with EEPROM Memory in SOT-23-6 (2009), Report no: MCP4725, Microchip Technology Inc., California.
- [2] 3-Phase AC Motor Control with V/Hz speed Closed Loop Using the 56F800/E (2005), Freescale Semiconductor Application Note, Denver, Colorado.
- [3] A Virtual Floating Point Engine, C28x Iqmath Library (2009), Texas Instruments, Dallas, Texas.
- [4] AC Drives Using PWM Techniques (2000), Report no: WP002A, Rockwell International Co., USA.
- [5] Akin, B., Clearman, C. (2010), Digital Motor Control Methodology for C2000TM Real-Time Control Microcontrollers, Report no: SMY001B, Texas Instruments Inc., Texas.
- [6] Alter, M.D. (2008), Using PWM Output as a Digital-to-Analog Converter on a TMS320F280x Digital Signal Controller, Report no: SPRAA88A, Texas Instruments Inc., Texas.
- [7] Azız, A.H.N. (2006), Three-Phase Squirrel-Cage Induction Motor Drive Analysis Using LABVIEW, Master of Science Thesis, Electrical Power Engineering, University of South Australia.
- [8] Bakan, F.A., et. al. (2003), Doğrudan Moment Kontrollü Bir Asenkron Motor Sürücüsünde Stator Akısı Tahmininin İyileştirilmesi, Elektrik-Elektronik-Bilgisayar Mühendisliği 10. Ulusal Kongresi ve Fuarı Bildirileri (18-21 Eylül), İstanbul 168-171.
- [9] Bakan, F.A., et. al. (2003), Doğrudan Moment Kontrollü Bir Asenkron Motor Sürücüsünde Anahtarlama Frekansının İncelenmesi, Elektrik-Elektronik-Bilgisayar Mühendisliği 10. Ulusal Kongresi ve Fuarı Bildirileri (18-21 Eylül), İstanbul 160-163.
- [10] Blake, C., Bull, C. (2006), IGBT or MOSFET: Choose Wisely, International Rectifier.
- [11] Bowling, S. (2005), An Introduction to AC Induction Motor Control Using the dsPIC30F MCU, Report no: AN984, Microchip Technology Inc., California.
- [12] Examples of Application Circuits (2004), Fuji Electric Device Technology Co.
- [13] Figoli, D. (1999), Creating a Sine Modulated PWM Signal Using the TMS320F240 EVM, Report no: SPRA411, Texas Instruments Inc., Texas.

- [14] Figoli, D. (1999), Generating a PWM Signal Modulated by an Analog Input Using the TMS320F240 EVM, Report no: SPRA413, Texas Instruments Inc., Texas.
- [15] Heustess, L. (2012), Programming TMS320x28xx and 28xxx Peripherals in C/C++, Report no: SPRAA85C, Texas Instruments Inc., Dallas, Texas.
- [16] Ice, C., Akin, B. (2009), Designing High-Performance and Power-Efficient Motor Control Systems, Report no: SPRT528, Texas Instruments Inc., Texas.
- [17] IGBT IPM R-Series 1200V Class, Report no: 7MBP50RJ120, Fuji Electric Device Technology Co.
- [18] Jaber, K., Fakhfakh, A., Neji, R. (2012), Comparison of SPWM and SVPWM Control of Electrical Vehicle in VHDL-AMS (21-24 March), Sciences of Electronics, Technologies of Information and Telecommunications, Tunisia, 1-6.
- [19] Jyang, Y.J. (1998), A CPLD-Based Voltage/Current Vector Controller for 3-Phase PWM Inverters, Power Electronics Specialists Conference, Fukuoka, 262-268, Vol 1.
- [20] Khluabwannarat, P. et.al. (2007), The Result Analysis of the Electrical Power and Temperature of 3-Phase Induction Motor Supplied by the PWM Inverter, The 8th International Power Engineering Conference, Singapore, 1197-1202.
- [21] Kohlrusz, G., Fodor, D. (2011), Comparison of Scalar and Vector Control Strategies of Induction Motors, Hungarian Journal of Industrial Chemistry, 265-270. Vol. 39(2).
- [22] Lee, J.J.et.al. (2003), Finite Element Analysis of 3-Phase Induction Motor with PWM Inverter, International Conference on Electrical Machines and Systems, China, 744-746, Vol 2.
- [23] Li, X., Duke, R., Round, S. (1999), Development of a Three-Phase Three-Level Inverter for an Electrical Vehicle, Australasian Universities Power Engineering Conference, Australia 247-251.
- [24] Maswood, A.I., Rahman, M.A. (2000), Performance of 3-Phase Induction Motor Fed from Improved Delta PWM Voltage Source Inverter, Power Engineering Society Winter Meeting, 381-386.
- [25] Mevey, R.J. (2009), Sensorless Field Oriented Control of Brushless Permanent Magnet Synchronous Motors, Master of Science Thesis, Kansas State University, Manhattan, Kansas.
- [26] Mohan, N., Undeland, T.M., Robbins, W.P. (1995), Power Electronics, John Wiley & Sons Inc., New York, 399-432.
- [27] Neacsu, O.D. (2001), Space Vector Modulation – An Introduction, IECON'01: The 27th Annual Conference of the IEEE Industrial Electronics Society, 1583-1592.
- [28] Nene, H. (2006), Using the Enhanced Pulse Width Modulator (ePWM) Module for 0% to 100% Duty Cycle Control, Report no: SPRAA11, Texas Instruments Inc., Texas.

- [29] Ogata, K. (2002), Modern Control Engineering, Prentice Hall, New Jersey, 682-684, 827-839.
- [30] Panda, S., Mishra, A., Srinivas, B. (2009), Control of Voltage source Inverters Using PWM/SVPWM for Adjustable Speed Drive Applications, Master of Science Thesis, National Institute of Technology Rourkela, Orissa.
- [31] Patakor, A.F., Sulaiman, M., Ibrahim, Z. (2011), Comparison Performance of Induction Motor Using SVPM and Hysteresis Current Controller, Journal of Theoretical and Applied Information Technology, 10-17. Vol.30 No.1.
- [32] Patil, M.P., Kurkute, L.S. (2006), Speed Control of Three Phase Induction Motor Using Single Phase Supply Along with Active Power Factor Correction, 23-32. Vol. 6.
- [33] Sensor Field Oriented Control (IFOC) of Three-Phase AC Induction Motors Using ST10F276 (2006), Report No: AN2388, STMicroelectronics.
- [34] Shet, K.S.M., Yaragatti, R.K.U. (2007), Design of Computer Application for 3 Phase Vector Control Induction Motor Drive, IET-UK International Conference on Information and Communication Technology in Electrical Sciences, India, 315-322.
- [35] Sowmmiya, U., Jamuna, V. (2010) Voltage Control Scheme for Three Phase SVM Inverter Fed Induction Motor Drive Systems, The Annals of "Dunarea De Jos" University of Galati Fascicle, 48-53. Vol.33.
- [36] Steki, P. (2007), 3-Phase AC Induction Vector Control Drive with Single Shunt Current Sensing Designer Reference Manual, Report No: DRM092, Freescale Semiconductor, Denver, Colorado.
- [37] SVM Space Vector Modulation, Improved Output Performance Through Advanced Inverter Control (2003), GE Industrial Systems, Switzerland.
- [38] Şimşek, G. (2004), Sensorless Direct Field Oriented Control of Induction Machine By Flux and Speed Estimation Using Model Reference Adaptive System, Master of Science Thesis, METU, Ankara.
- [39] TMS320x280x, 2801x, 2804x Enhanced Pulse Width Modulator (ePWM) Module Reference Guide (2009), Report No: SPRU791F, Texas Instruments Inc., Dallas, Texas.
- [40] TMS320x2802x, 2803x Piccolo Analog to Digital Converter and Comparator Reference Guide (2008), Texas Instruments, Dallas, Texas.
- [41] TMS320x2802x, 2803x Piccolo Inter-Integrated Circuit Module (2008), Texas Instruments, Dallas, Texas.
- [42] Ün, E. (2007), Common Mode Voltage and Current Reduction in Voltage Source Inverter Driven Three Phase AC Motors, Master of Science Thesis, Electrical and Electronics Engineering, METU, Ankara.
- [43] Wang, X. (2001), Modeling and Implementation of Controller for Switched Reluctance Motor with AC Small Signal Model, Master of Science Thesis, Virginia Polytechnic Institute and State University, Blacksburg, Virginia.

[44] Win, T. et. al. (2008), Analysis of Variable Frequency Three Phase Induction Motor Drive, World Academy of Science, Engineering and Technology, 647-651, Vol. 42.

[45] Yedamale, P. (2002), Speed Control of 3-Phase Induction Motor Using PIC18 Microcontrollers, Report no: AN848, Microchip Technology Inc.

[46] Yu, Z. (1999), Space-Vector PWM with TMS320C24x/F24x Using Hardware and Software Determined Switching Patterns, Report no: SPRA524, Texas Instruments Inc., Texas.

[47] Yu, Z., Figoli, D. (1998), AC Induction Motor Control Using Constant V/Hz Principle and Space Vector PWM Technique with TMS320C240, Report no: SPRA284A, Texas Instruments Inc., Texas.

[48] Zhou, K., Wang, D. (2002), Relationship Between Space-Vector Modulation and Three-Phase Carrier-Based PWM: A Comprehensive Analysis, IEEE Transactions on Industrial Electronics, 186-195, Vol.49, No.1.

[49] ACS355 Drives User's Manual (2012), Report No: 3AUA0000066143, ABB, Zurich, Switzerland.

CURRICULUM VITAE

PERSONAL INFORMATION

Surname, Name: Öz, Habib Özer
Nationality: Turkish (TC)
Date and Place of Birth: 25 May 1983 , Erzurum
Marital Status: Single
Phone:+90 312 210 00 10
Fax: +90 312 210 00 11
email: habibozeroz@gmail.com

EDUCATION

Degree	Institution	Year of Graduation
MS	Çankaya University Electronic and Communication Engineering	2012
BS	Baskent University Electric and Electronic Engineering	2007
High School	Çankaya Milli Piyango Anadolu Lisesi, Ankara	2001

WORK EXPERIENCE

Year	Place	Enrollment
2007-Present	Yıldırım Elektronik LTD. ŞTİ	R&D Engineer

FOREIGN LANGUAGES

Advanced English

PUBLICATIONS

1. ELSEVIER ScienceDirect Procedia Social and Behavioral Sciences 1 (2009)
2865-2870 World Conference on Educational Sciences 2009 A General
Purpose Computer Interface Unit for Electrical and Electronics Education

HOBBIES

Basketball, American Football